HYDJET++:

Ultrarelativistic heavy ion collisions – a hot cocktail of hydrodynamics, resonances and jets

L. Bravina

in collaboration with

H. Brusheim Johansson, J. Crkovska, G. Eyyubova, V. Korotkih, I. Lokhtin, L. Malinina, S. Petrushanko, A. Snigirev and E. Zabrodin

XI-th Quark Confinement and the Hadron Spectrum

St.-Petersburg, Russia, 09.09.2014

Outline

I. HYDJET++ model (hydro + jets)
II. Description of elliptic flow in relativistic heavy ion collisions
III. Influence of resonance decays
IV. NCQ-scaling at RHIC and LHC
V. Triangular flow
VI. Higher flow harmonics
VII. Conclusions

I. HYDJET++ =
FASTMC + HYDJET

Relativistic heavy ion event generator HYDJET++

HYDJET++ (HYDrodynamics + JETs) - event generator to simulate heavy ion event by merging of two independent components (soft hydro-type part + hard multi-partonic state, the latter is based on PYQUEN - PYthia QUENched routine).

http://cern.ch/lokhtin/hydjet++ *(latest version 2.1)*

[1] I. Lokhtin, L. Malinina, S. Petrushanko, A. Snigirev, I. Arsene, K. Tywoniuk, Comp. Phys. Comm. 180 (2009) 77

[2] I. Lokhtin, A. Belyaev, L. Malinina, S. Petrushanko, E. Rogochaya, A. Snigirev, Eur. Phys. J. C 72 (2012) 2045

[3] L. Bravina, H. Brusheim Johansson, G. Eyyubova, V. Korotkikh, I. Lokhtin, L. Malinina, S. Petrushanko, A. Snigirev, E. Zabrodin, Eur. Phys. J. C 74 (2014) 2807

HYDJET++ (soft): hydrodynamics with resonances

Soft (hydro) part of HYDJET++ is based on the adapted FAST MC model:
Part I: N.S.Amelin, R.Lednisky, T.A.Pocheptsov, I.P.Lokhtin, L.V.Malinina, A.M.Snigirev, Yu.A.Karpenko, Yu.M.Sinyukov, Phys. Rev. C 74 (2006) 064901
Part II: N.S.Amelin, R.Lednisky, I.P.Lokhtin, L.V.Malinina, A.M.Snigirev, Yu.A.Karpenko, Yu.M.Sinyukov, I.C.Arsene, L.Bravina, Phys. Rev. C 77 (2008) 014903

- fast HYDJET-inspired MC procedure for soft hadron generation
  multiplicities are determined assuming thermal equilibrium
- hadrons are produced on the hypersurface represented by a parameterization of relativistic hydrodynamics with given freeze-out conditions
- chemical and kinetic freeze-outs are separated
- decays of hadronic resonances are taken into account (360 particles from SHARE data table) with severely modified decayer
- written within ROOT framework (C++)
- contains 16 free parameters (but this number may be reduced to 9)

HYDJET++ (soft): main physics assumptions

A hydrodynamic expansion of the fireball is supposed to end by a sudden system breakup at given T and chemical potentials. Momentum distribution of produced hadrons keeps the thermal character of the equilibrium distribution.

Cooper-Frye formula: $$p^0 \frac{d^3 N_i}{d^3 p} = \int_{\sigma(x)} d^3\sigma_\mu(x) p^\mu f_i^{eq}(p^\nu u_\mu(x); T, \mu_i)$$

- HYDJET++ avoids straightforward 6-dimensional integration by using the special simulation procedure (like HYDJET): momentum generation in the rest frame of fluid element, then Lorentz transformation in the global frame → uniform weights → effective von-Neumann rejection-acception procedure.

Freeze-out surface parameterizations

1. The Bjorken model with hypersurface $\tau = (t^2 - z^2)^{1/2} = const$
2. Linear transverse flow rapidity profile $\rho_u = \frac{r}{R}\rho_u^{\max}$
3. The total effective volume for particle production at

- $$V_{eff} = \int_{\sigma(x)} d^3\sigma_\mu(x) u^\mu(x) = \tau \int_0^R \gamma_r r dr \int_0^{2\pi} d\phi \int_{\eta_{\min}}^{\eta_{\max}} d\eta = 2\pi\tau\Delta\eta \left(\frac{R}{\rho_u^{\max}}\right)^2 (\rho_u^{\max}\sinh\rho_u^{\max} - \cosh\rho_u^{\max} + 1)$$

HYDJET++ (soft): hadron multiplicities

1. The hadronic matter created in heavy-ion collisions is considered as a hydrodynamically expanding fireball with EOS of an ideal hadron gas.

$$N_i = \rho_i(T, \mu_i) V_{eff}$$

2. "Concept of effective volume" T=const and μ=const: the total yield of particle species is

$$T(\mu_B) = a - b\mu_B - c\mu_B^4; \quad \mu_B(\sqrt{s_{NN}}) = \frac{d}{1 + e\sqrt{s_{NN}}}$$

3. Chemical freeze-out : T, $\mu_i = \mu_B B_i + \mu_S S_i + \mu_c C_i + \mu_Q Q_i$; T, μ_B –can be fixed by particle ratios, or by phenomenological formulas

$$f_i^{eq}(p^{0*}; T, \mu_i) = \frac{1}{(2\pi)^3} \frac{g_i}{\exp([p^{0*} - \mu_i]/T) \pm 1}$$

4. Chemical freeze-out: all macroscopic characteristics of particle system are determined via a set of equilibrium distribution functions in the fluid element rest frame:

$$\rho_i^{eq}(T, \mu_i) = \int_0^\infty d^3\vec{p}^{\,*} f_i^{eq}(p^{0*}; T(x^*), \mu(x^*)_i) = 4\pi \int_0^\infty dp^* p^{*2} f_i^{eq}(p^{0*}; T, \mu_i)$$

HYDJET++ (soft): thermal and chemical freeze-outs

1. The particle densities at the chemical freeze-out stage are too high to consider particles as free streaming and to associate this stage with the thermal freeze-out

2. Within the concept of chemically frozen evolution, the conservation of the particle number ratios from the chemical to thermal freeze-out is assumed:

$$\frac{\rho_i^{eq}(T^{ch},\mu_i^{ch})}{\rho_\pi^{eq}(T^{ch},\mu_\pi^{ch})} = \frac{\rho_i^{eq}(T^{th},\mu_i^{th})}{\rho_\pi^{eq}(T^{th},\mu_\pi^{th})}$$

3. The absolute values of $\rho_i^{eq}(T^{th},\mu_i^{th})$ are determined by the choice of the free parameter of the model: effective pion chemical potential $\mu_\pi^{eff,th}$ at T^{th}
For hadrons heavier than pions the Boltzmann approximation is assumed:

$$\mu_i^{th} = T^{th}\ln\left(\frac{\rho_i^{eq}(T^{ch},\mu_i^{ch})}{\rho_i^{eq}(T^{th},\mu_i=0)}\frac{\rho_\pi^{eq}(T^{th},\mu_\pi^{eff,th})}{\rho_\pi^{eq}(T^{ch},\mu_i^{ch})}\right)$$

Particle momentum spectra are generated on the thermal freeze-out hypersurface, the hadronic composition at this stage is defined by the parameters of the system at chemical freeze-out

HYDJET++ (soft): input parameters

1-5. Thermodynamic parameters at chemical freeze-out: T_{ch} , {μ_B, μ_S, μ_C, μ_Q} (option to calculate T_{ch}, μ_B and μ_s using phenomenological parameterization $\mu_B(\sqrt{s})$, $T_{ch}(\mu_B)$ is foreseen).

6-7. Strangeness suppression factor $\gamma_S \leq 1$ and charm enchancement factor $\gamma_c \geq 1$ (options to use phenomenological parameterization $\gamma_S(T_{ch}, \mu_B)$ and to calculate γ_c are foreseen).

8-9. Thermodynamical parameters at thermal freeze-out: T_{th} , and μ_π- effective chemical potential of positively charged pions.

10-12. Volume parameters at thermal freeze-out: proper time τ_f , its standard Deviation (emission duration) $\Delta\tau_f$, maximal transverse radius R_f .

13. Maximal transverse flow rapidity at thermal freeze-out ρ_u^{max} .

14. Maximal longitudinal flow rapidity at thermal freeze-out η^{max} .

15. Flow anisotropy parameter: $\delta(b) \rightarrow u^\mu = u^\mu(\delta(b),\varphi)$

16. Coordinate anisotropy:

$$\varepsilon(b) \rightarrow R_f(b)=R_f(0)[V_{eff}(\varepsilon(0),\delta(0))/V_{eff}(\varepsilon(b),\delta(b))]^{1/2}[N_{part}(b)/N_{part}(0)]^{1/3}$$

For impact parameter range bmin-bmax:

$$V_{eff}(b)=V_{eff}(0)N_{part}(b)/N_{part}(0), \quad \tau_f(b)=\tau_f(0)[N_{part}(b)/N_{part}(0)]^{1/3}$$

HYDJET++ (hard): PYQUEN (PYthia QUENched)

Initial parton configuration
PYTHIA6.4 w/o hadronization: mstp(111)=0

↓

Parton rescattering & energy loss (collisional, radiative) + emitted g
PYQUEN rearranges partons to update ns strings

↓

Parton hadronization and final particle formation
PYTHIA6.4 with hadronization: call PYEXEC

Three model parameters: initial QGP temperature T0, QGP formation time τ0 and number of active quark flavors in QGP Nf
(+ minimal pT of hard process Ptmin)

I.P.Lokhtin, A.M.Snigirev, Eur. Phys. J. 45 (2006) 211 (latest version 1.5.1)

Parton rescattering and jet quenching

Collisional loss

(high momentum transfer approximation)

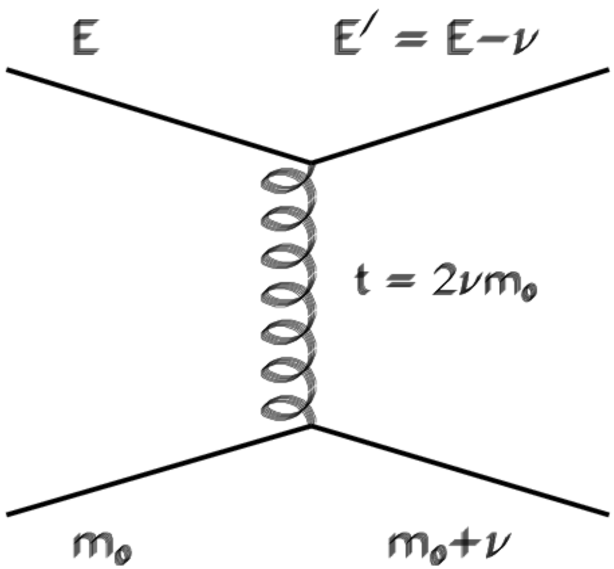

\+

Radiative loss

(BDMS model, coherent radiation)

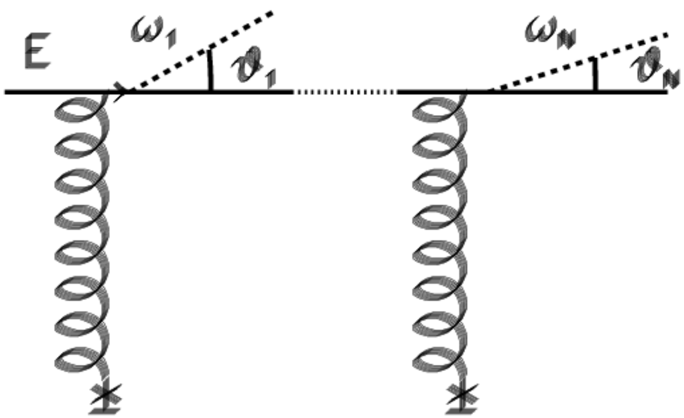

Strength of e-loss in PYQUEN is determined mainly by initial maximal temperature T0 of hot matter in central (b=0) PbPb collisions (depends also on formation time τ_0 and # of quark flavors N_f)

PYQUEN: physics frames

General kinetic integral equation:

$$\Delta E(L,E)=\int_0^L dx \frac{dP}{dx}(x)\lambda(x)\frac{dE}{dx}(x,E), \quad \frac{dP}{dx}(x)=\frac{1}{\lambda(x)}\exp(-x/\lambda(x))$$

1. Collisional loss and elastic scattering cross section:

$$\frac{dE}{dx}=\frac{1}{4T\lambda\sigma}\int_{\mu_D^2}^{t_{max}} dt\frac{d\sigma}{dt}t, \quad \frac{d\sigma}{dt}\simeq C\frac{2\pi\alpha_s^2(t)}{t^2}, \quad \alpha_S=\frac{12\pi}{(33-2N_f)\ln(t/\Lambda_{QCD}^2)}, \quad C=9/4(\%gg),1(gq),4/9(qq)$$

2. Radiative loss (BDMS):

$$\frac{dE}{dx}(m_q=0)=\frac{2\alpha_s C_F}{\pi\tau_L}\int_{E_{LPM}\sim\lambda_g\mu_D^2}^{E} d\omega\left[1-y+\frac{y^2}{2}\right]\ln\left|\cos(\omega_1\tau_1)\right|, \quad \omega_1=\sqrt{i\left(1-y+\frac{C_F}{3}y^2\right)\bar{k}\ln\frac{16}{\bar{k}}}, \quad \bar{k}=\frac{\mu_D^2\lambda_g}{\omega(1-y)}, \quad \tau_1=\frac{\tau_L}{2\lambda_g}, \quad y=\frac{\omega}{E}, \quad C_F=\frac{4}{3}$$

“dead cone” approximation for massive quarks:

$$\frac{dE}{dx}(m_q\neq 0)=\frac{1}{\left(1+(l\omega)^{3/2}\right)^2}\frac{dE}{dx}(m_q=0), \quad l=\left(\frac{\lambda}{\mu_D^2}\right)^{1/3}\left(\frac{m_q}{E}\right)^{4/3}$$

Nuclear geometry and QGP evolution

impact parameter b≡ $|O_1O_2|$ - transverse distance between nucleus centers

$$\varepsilon(r_1,r_2) \propto T_A(r_1) * T_A(r_2)$$ (T_A(b) - nuclear thickness function)

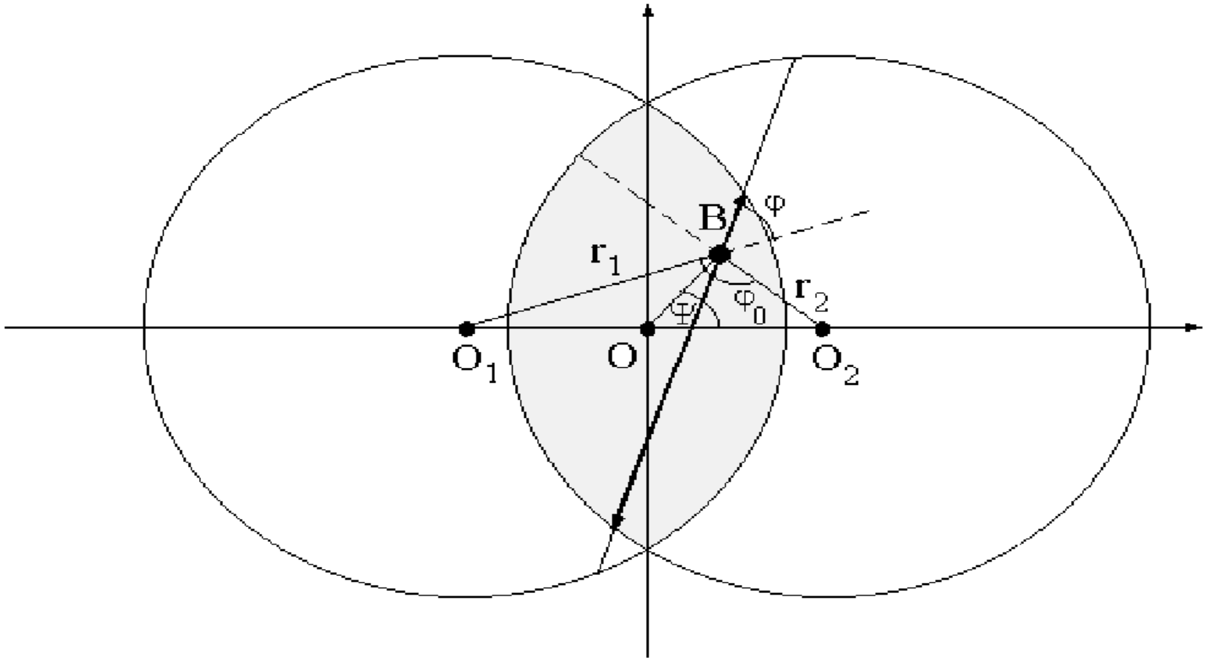

Space-time evolution of QGP, created in region of initial overlaping of colliding nuclei, is descibed by Lorenz-invariant Bjorken's hydrodynamics J.D. Bjorken, PRD 27 (1983) 140

Monte-Carlo simulation of parton rescattering and energy loss in PYQUEN

- Distribution over jet production vertex $V(r\cos\psi, r\sin\psi)$ at im.p. b

$$\frac{dN}{d\psi dr}(b)=\frac{T_A(r_1)T_A(r_2)}{\int_0^{2\pi} d\psi \int_0^{r_{max}} rdrT_A(r_1)T_A(r_2)}$$

- Transverse distance between parton scatterings $l_i=(\tau_{i+1}-\tau_i)\,E/p_T$

$$\frac{dP}{dl_i}=\lambda^{-1}(\tau_{i+1})\exp\left(-\int_0^{l_i}\lambda^{-1}(\tau_i+s)ds\right),\quad \lambda^{-1}=\sigma\rho$$

- Radiative and collisional energy loss per scattering

$$\Delta E_{tot,i}=\Delta E_{rad,i}+\Delta E_{col,i}$$

- Transverse momentum kick per scattering

$$\Delta k_{t,i}^2=\left(E-\frac{t_i}{2\mathrm{m}_{0i}}\right)^2-\left(p-\frac{E}{p}\frac{t_i}{2\mathrm{m}_{0i}}-\frac{t_i}{2\mathrm{p}}\right)^2-m_q^2$$

Monte-Carlo simulation of hard component (including nuclear shadowing) in HYDJET/HYDJET++

- Calculating the number of hard NN sub-collisions Njet (b, Ptmin, $\sqrt{s}$) with Pt>Ptmin around its mean value according to the binomial distribution.
- Selecting the type (for each of Njet) of hard NN sub-collisions (pp, np or nn) depending on number of protons (Z) and neutrons (A-Z) in nucleus A according to the formula: $Z=A/(1.98+0.015A^{2/3})$.
- Generating the hard component by calling PYQUEN njet times.
- Correcting the PDF in nucleus by the accepting/rejecting procedure for each of Njet hard NN sub-collisions: comparision of random number generated uniformly in the interval [0,1] with shadowing factor $S(r1,r2,x1,x2,Q2) \leq 1$ taken from the adapted impact parameter dependent parameterization based on Glauber-Gribov theory *(K.Tywoniuk et al., Phys. Lett. B 657 (2007) 170)*.

II. Elliptic flow in HYDJET++ : interplay of hydrodynamics and jets

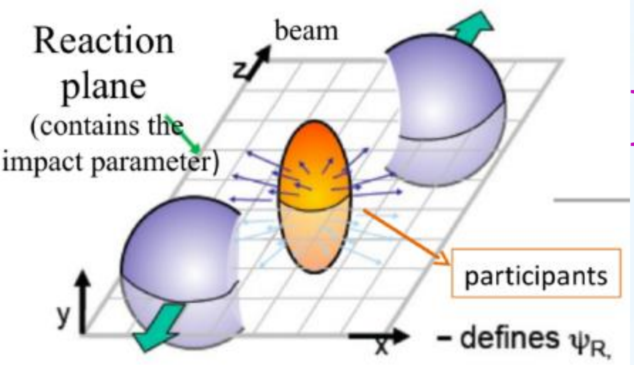

ELLIPTIC FLOW

Initial spatial anisotropy is converted to anisotropy in momentum space

Initial anisotropy

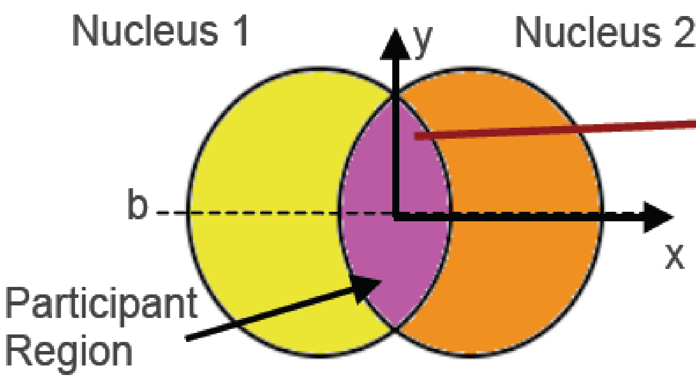

Pressure driven expansion

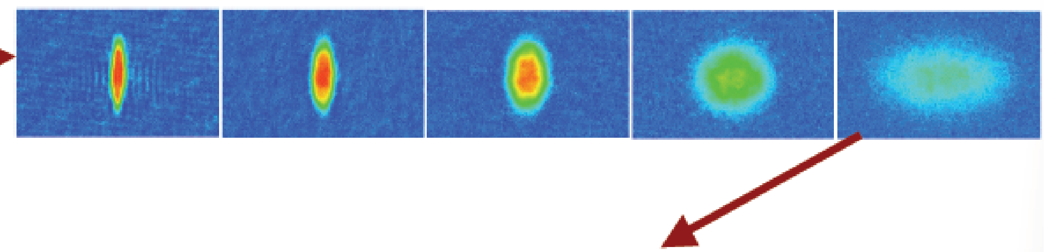

Final anisotropy

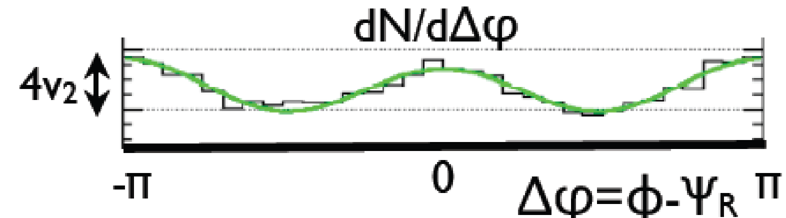

$$\frac{dN}{d\phi} = \frac{N}{2\pi}\left(1 + \sum 2v_n \cos\left(n(\phi - \psi_R)\right)\right)$$

S.Voloshin, Y.Zhang, Z.Phys.C70 (1996) 665

$$v_2 = \left\langle \cos\left(2(\phi - \underline{\psi_R})\right)\right\rangle \propto \varepsilon$$

Elliptic flow is quantified by the second Fourier coefficient (v_2) of the observed particle distribution

RHIC data vs. HYDJET++ model

Au+Au @ 200 AGeV

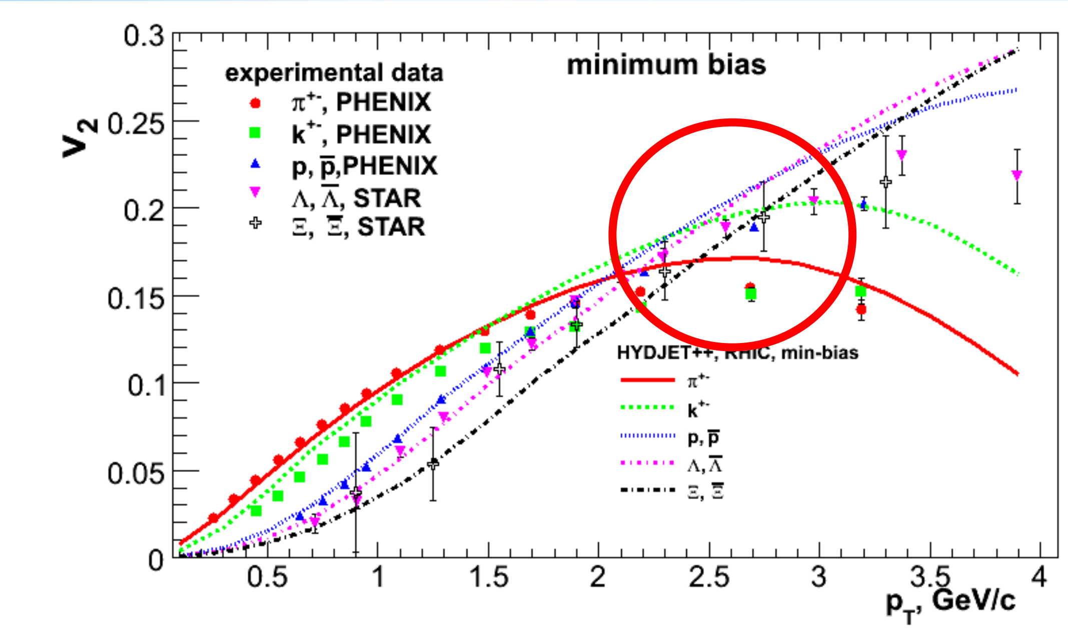

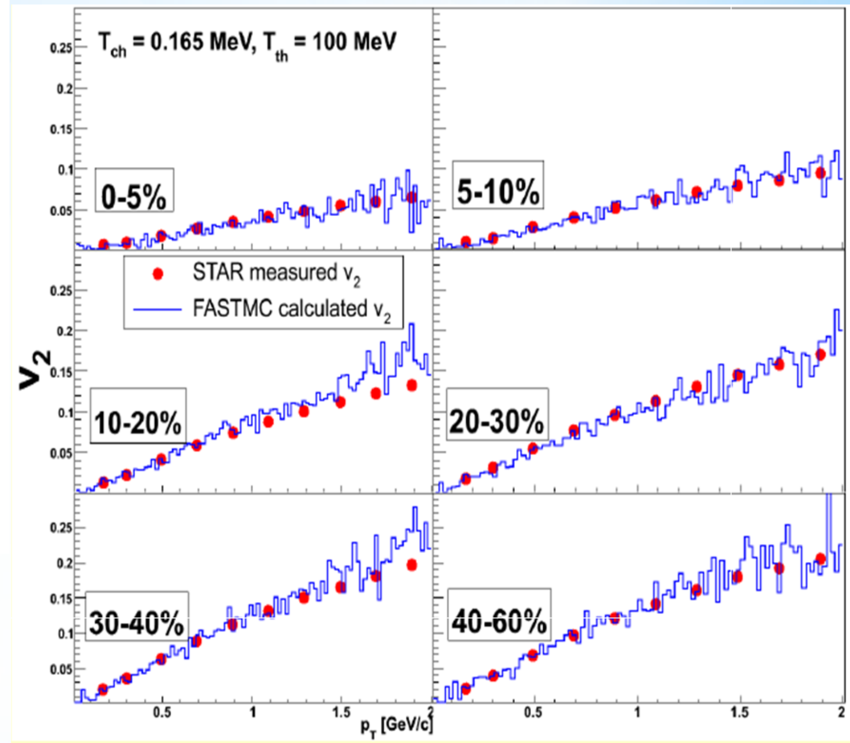

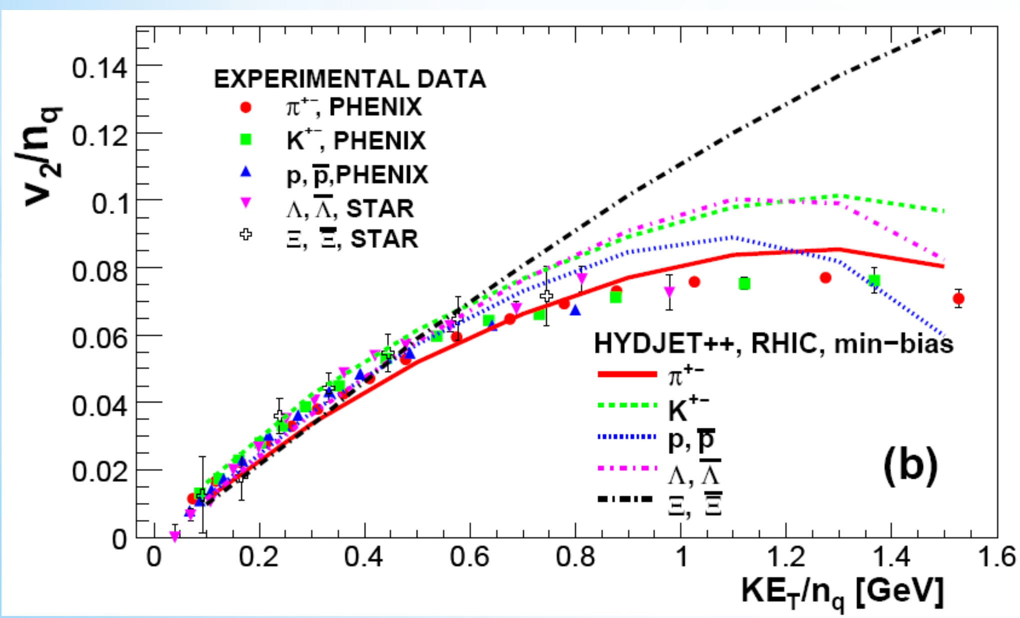

Elliptic flow

G. Eyyubova et al., PRC 80 (2009) 064907;
N.S. Amelin et al., PRC 77 (2008) 014903

V2 in HYDJET++ for different particles (centrality 30%)

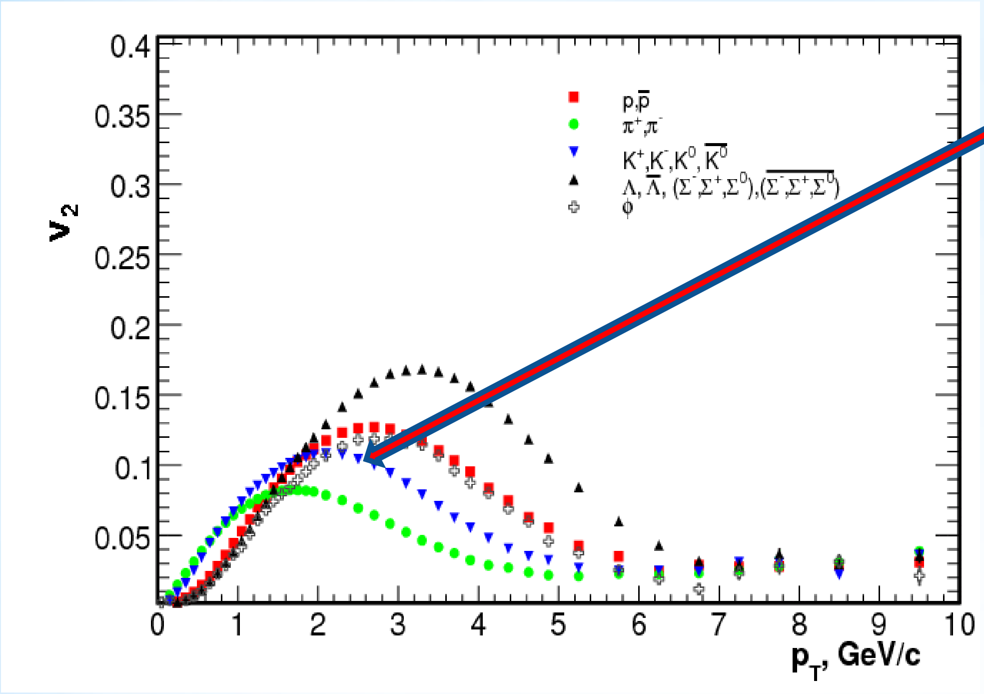

Mass ordering in soft pT regions then breaks.

Why?

Hydrodynamics gives mass ordering of v2.
The model possesses crossing of baryon and meson branches.

Hydrodynamics

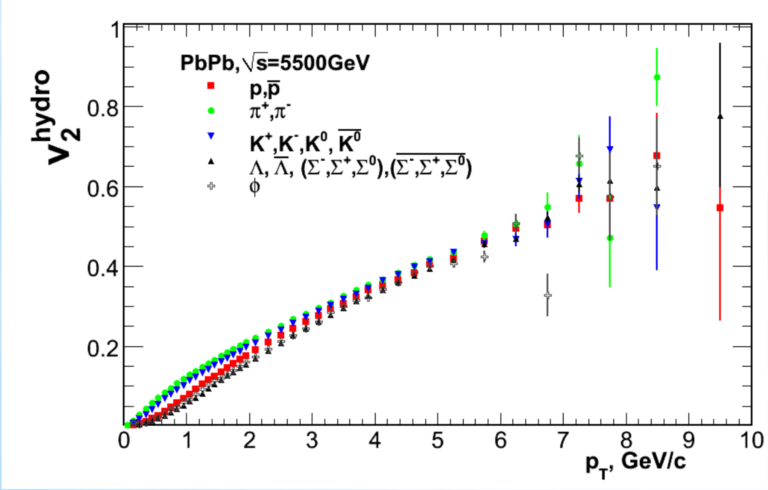

Jet part +quenching

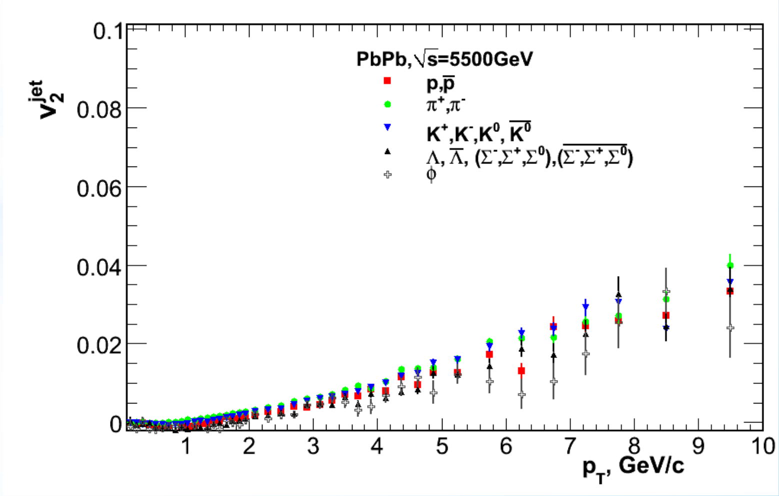

Interplay between hydrodynamics and jets

The pT specta of π, K, p, Λ with HYDJET++ model, √s=200GeV

The slope for the hydro part depends strongly on mass:

- the heavier the particle -- the harder the spectrum

The hydro part dies out earlier for light particles than for heavy ones

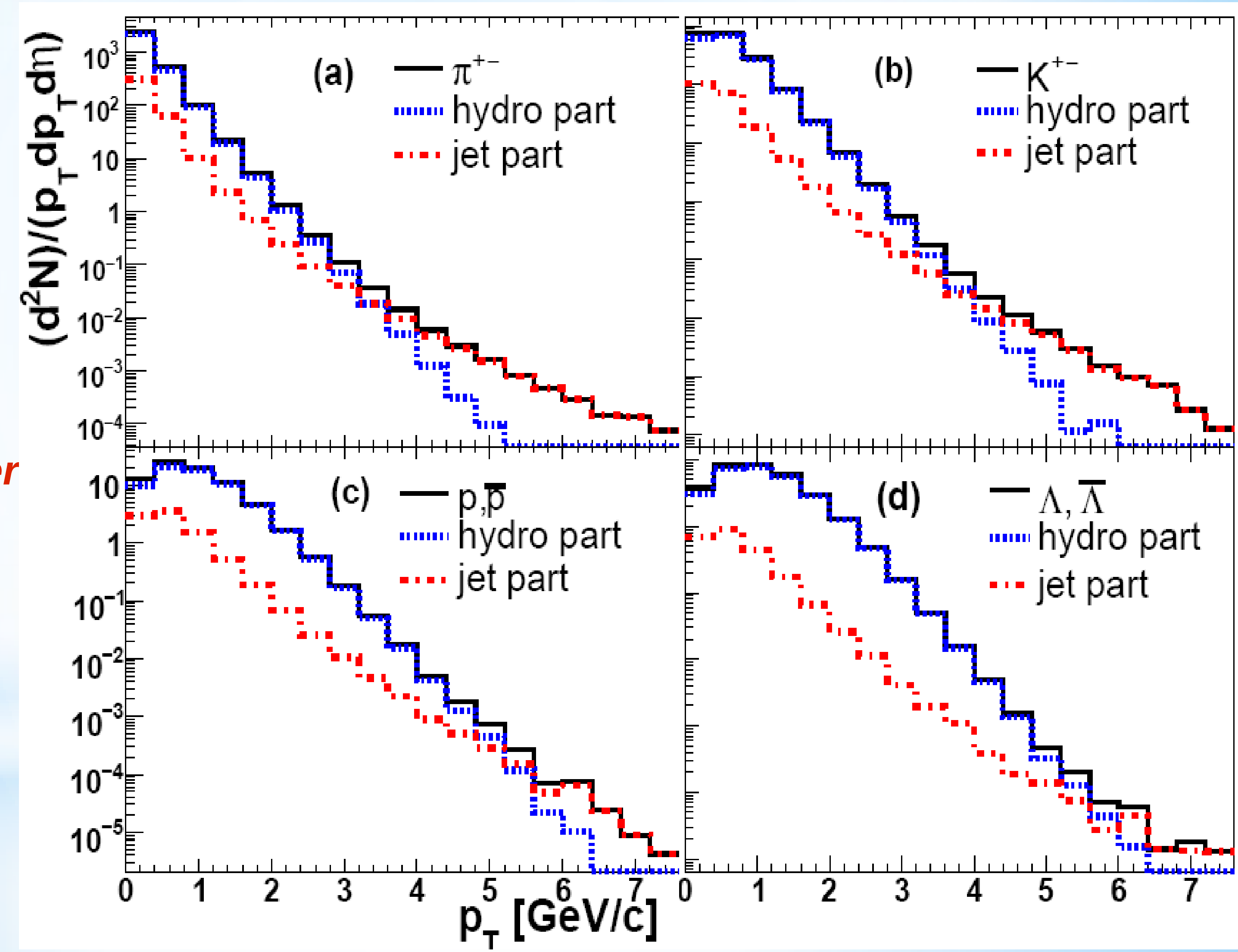

LHC data vs. HYDJET++ model

Elliptic flow

Pb+Pb @ 2.76 ATeV

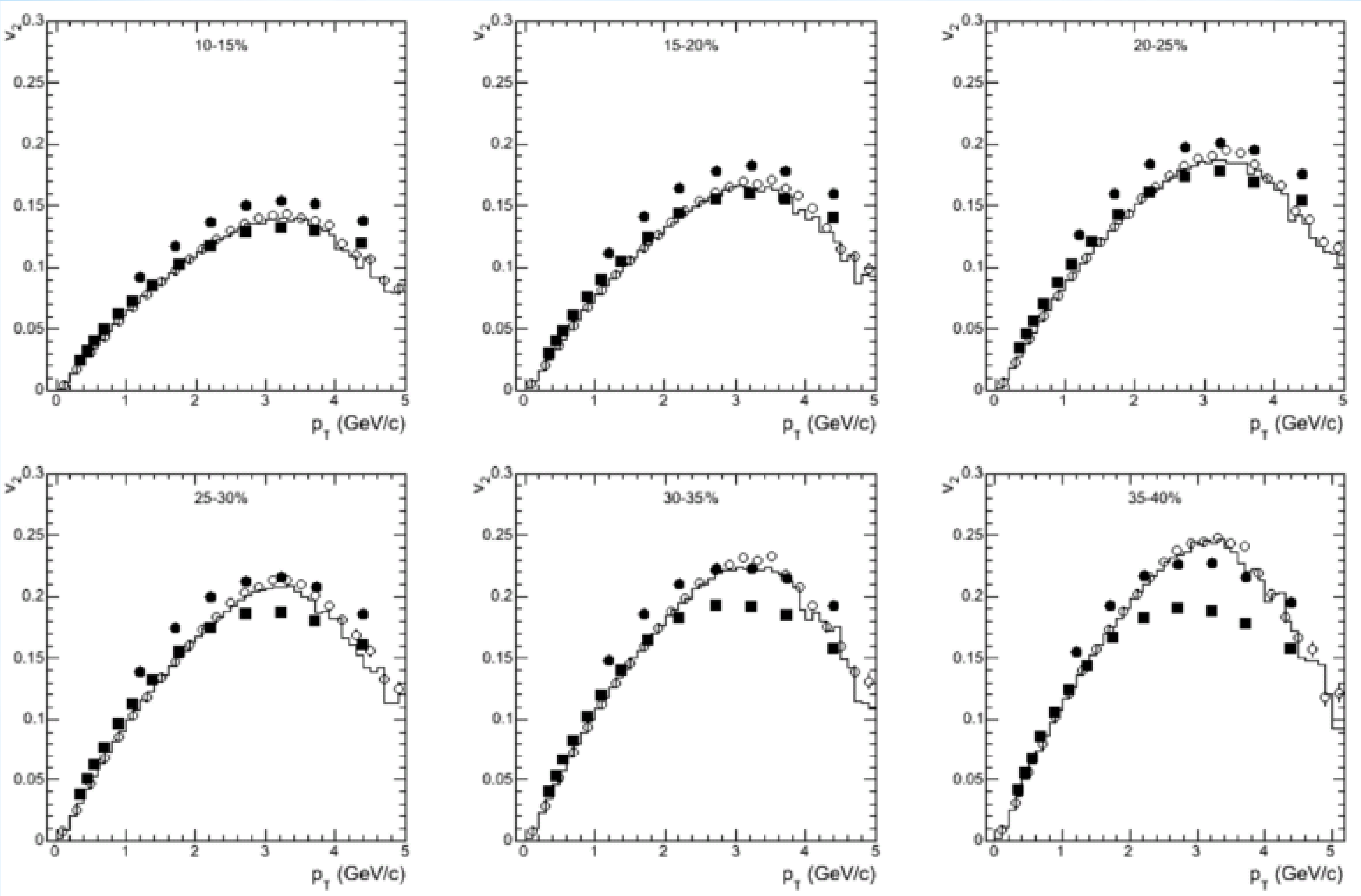

L. B. et al., Eur. Phys. J C74 (2014) 2807

Closed points: CMS data v2{2Part & LYZ};

Open points and histograms: HYDJET++ v2{EP & Psi2}

Ⅲ． Influence of resonance decays

Influence of resonance decays for different type of particles at LHC

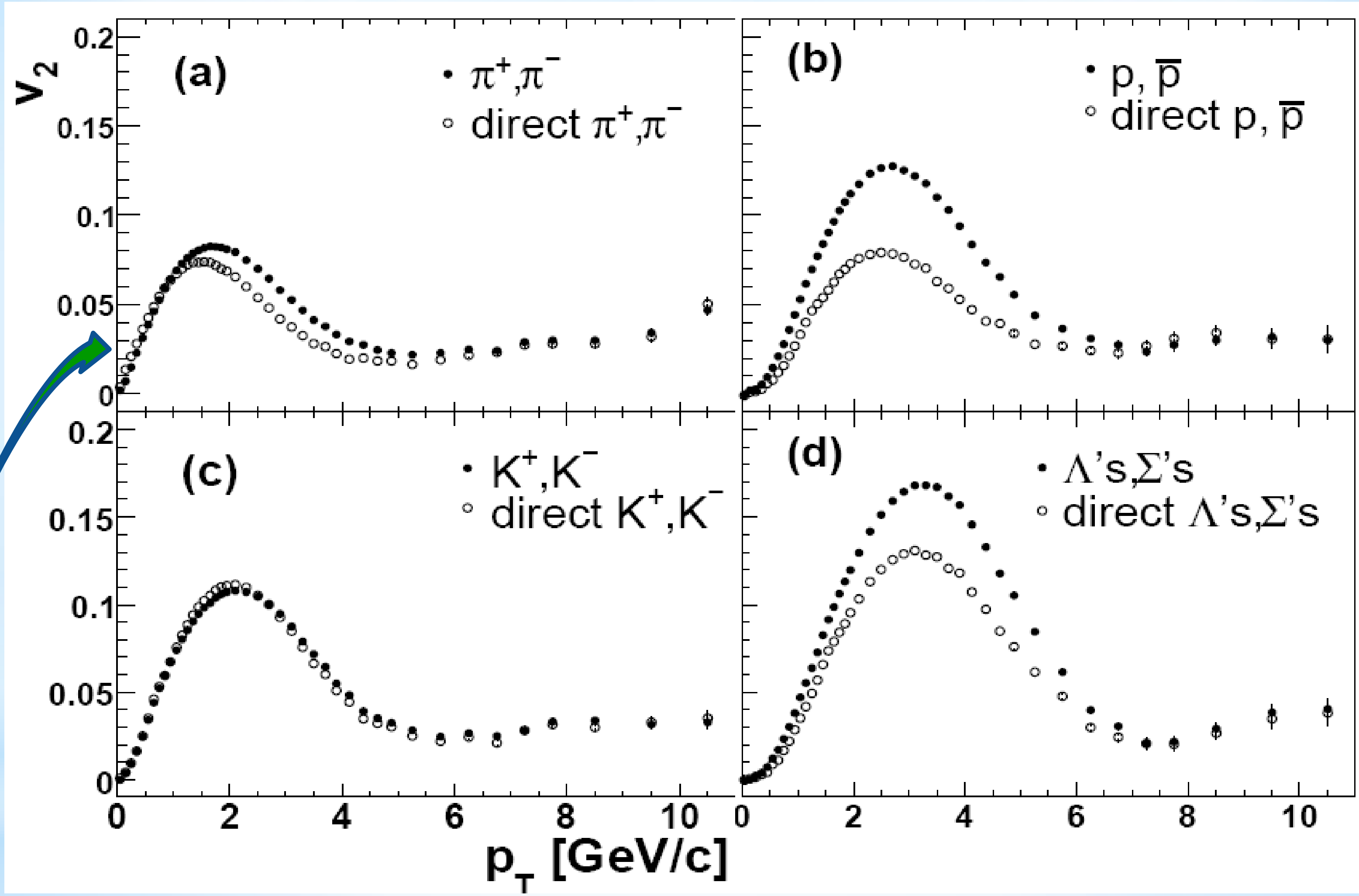

G. Eyyubova et al., PRC 80 (2009) 064907

Pions: the resulting flow is weaker at low-pt and larger at high-pt

Kaons: both flows almost coincide

Baryons: the resulting flow is stronger than the flow of direct particles

Transverse momentum of secondary particles

$\Delta \rightarrow \pi + p$

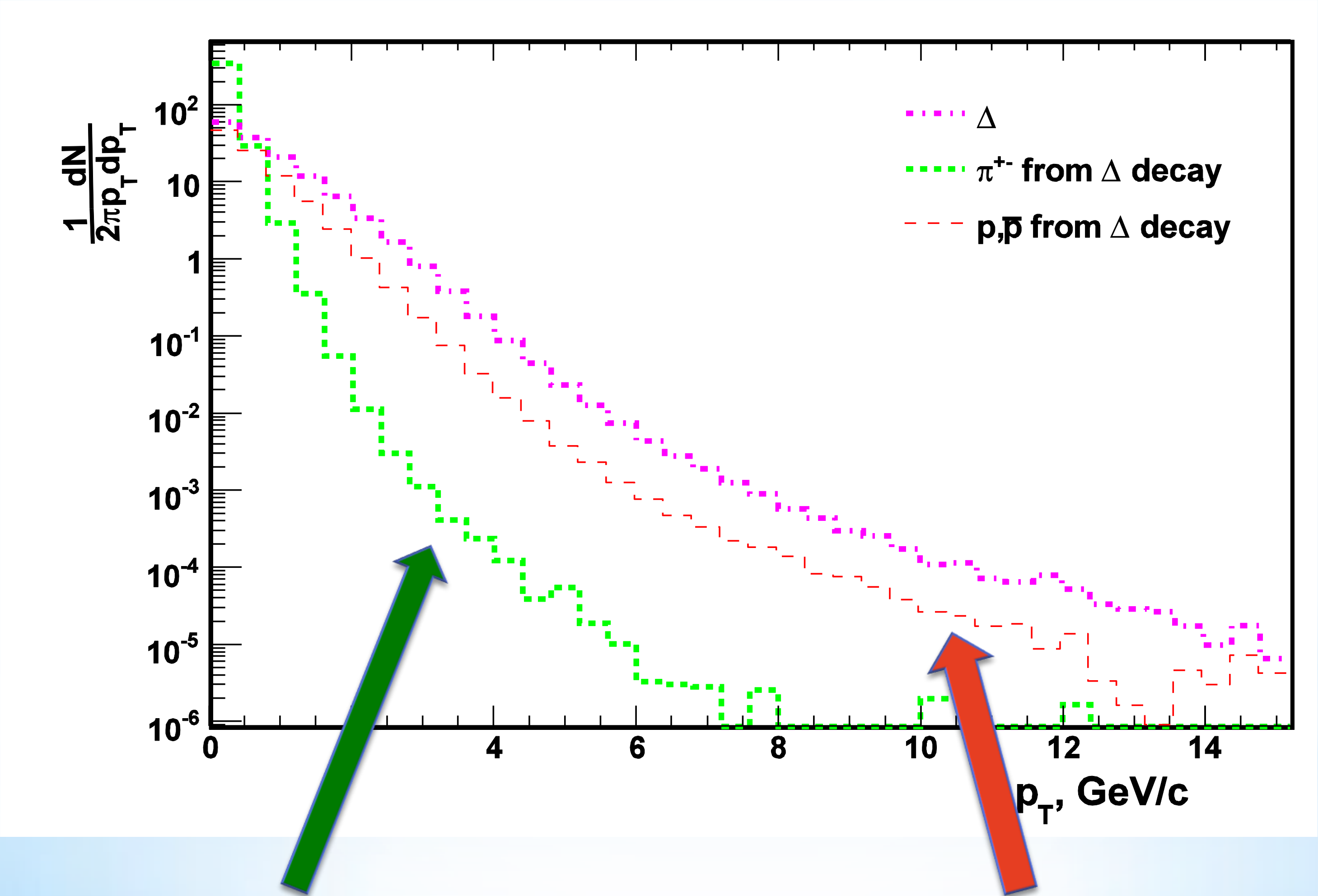

The secondary pion spectrum is much softer than proton spectrum

Elliptic flow of direct and secondary particles at LHC

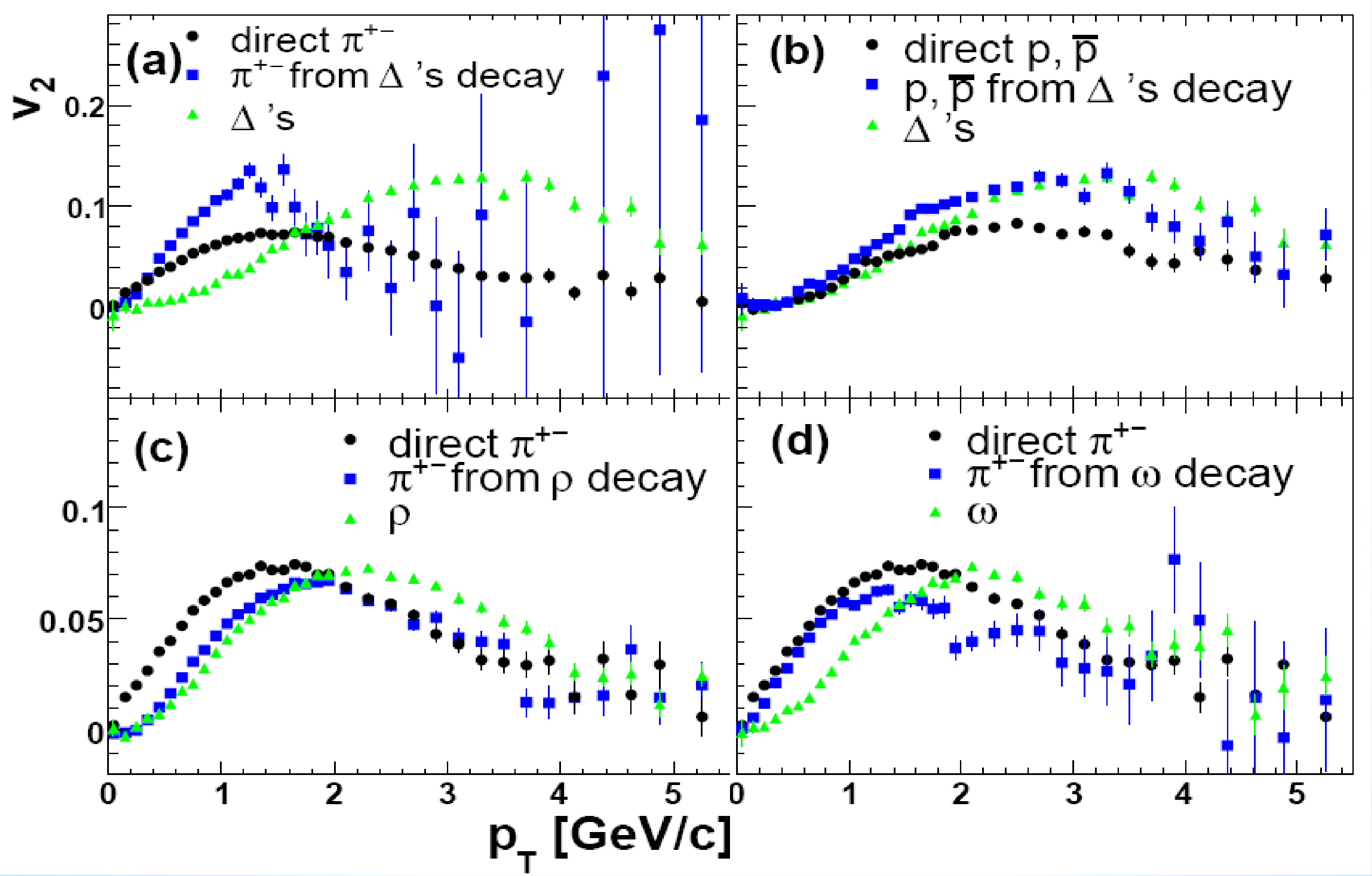

At low transverse momenta: pions from baryon resonances enhance the flow; pions from meson resonances reduce it

IV. Number-of-constituent-quark (NCQ) scaling

Number-of-constituent-quark scaling at RHIC

Direct particles: scaling is not good. All particles: KET/nq scaling

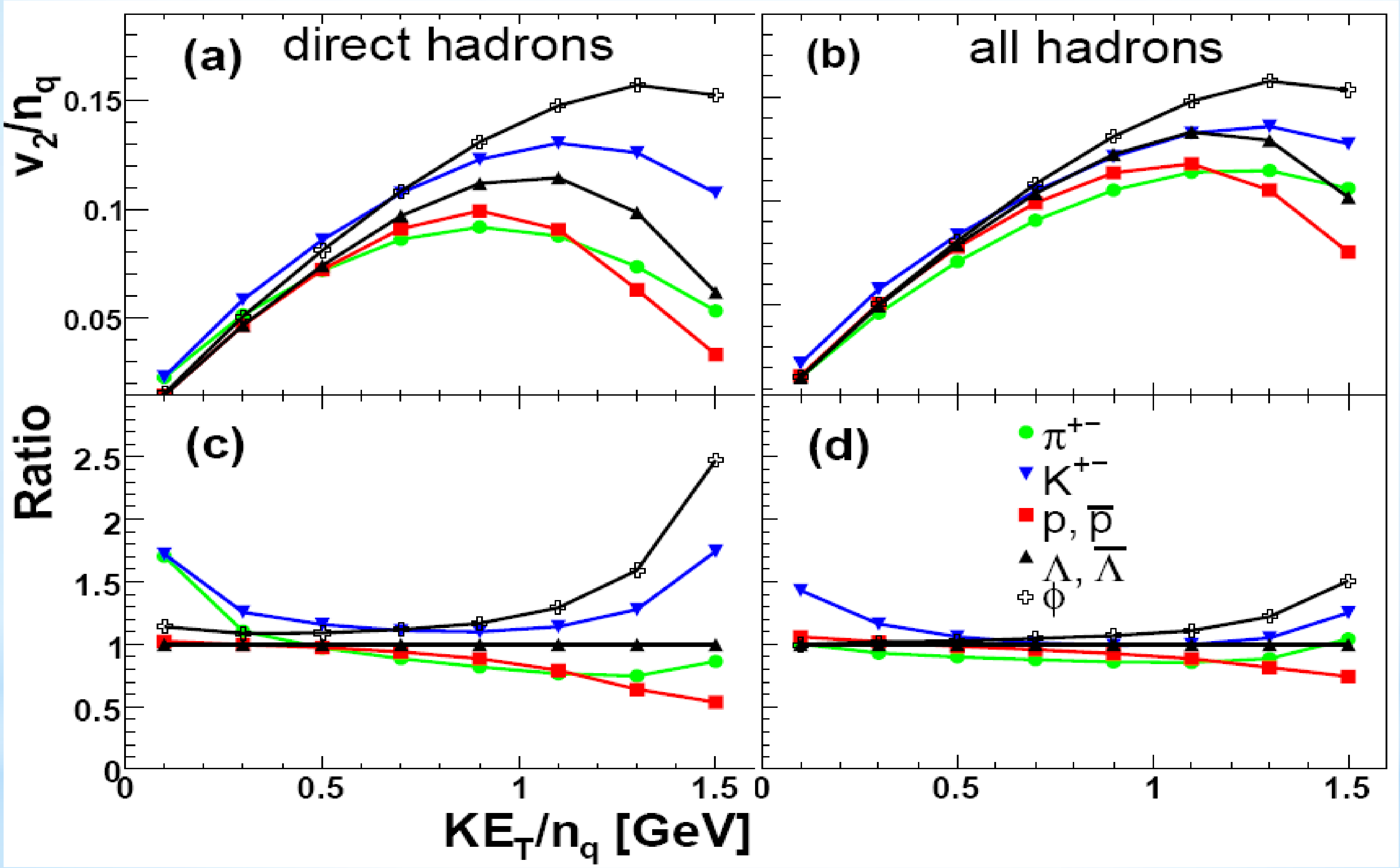

G.Eyyubova et al., PRC 80 (2009) 064907

One of the explanations of KET/nq scaling is partonic origin of the elliptic flow.

However, final state effects (such as resonance decays and jets) may also lead to appearance of the scaling

NCQ scaling at LHC

No scaling for direct particles

Appearance of the approximate scaling for all particles

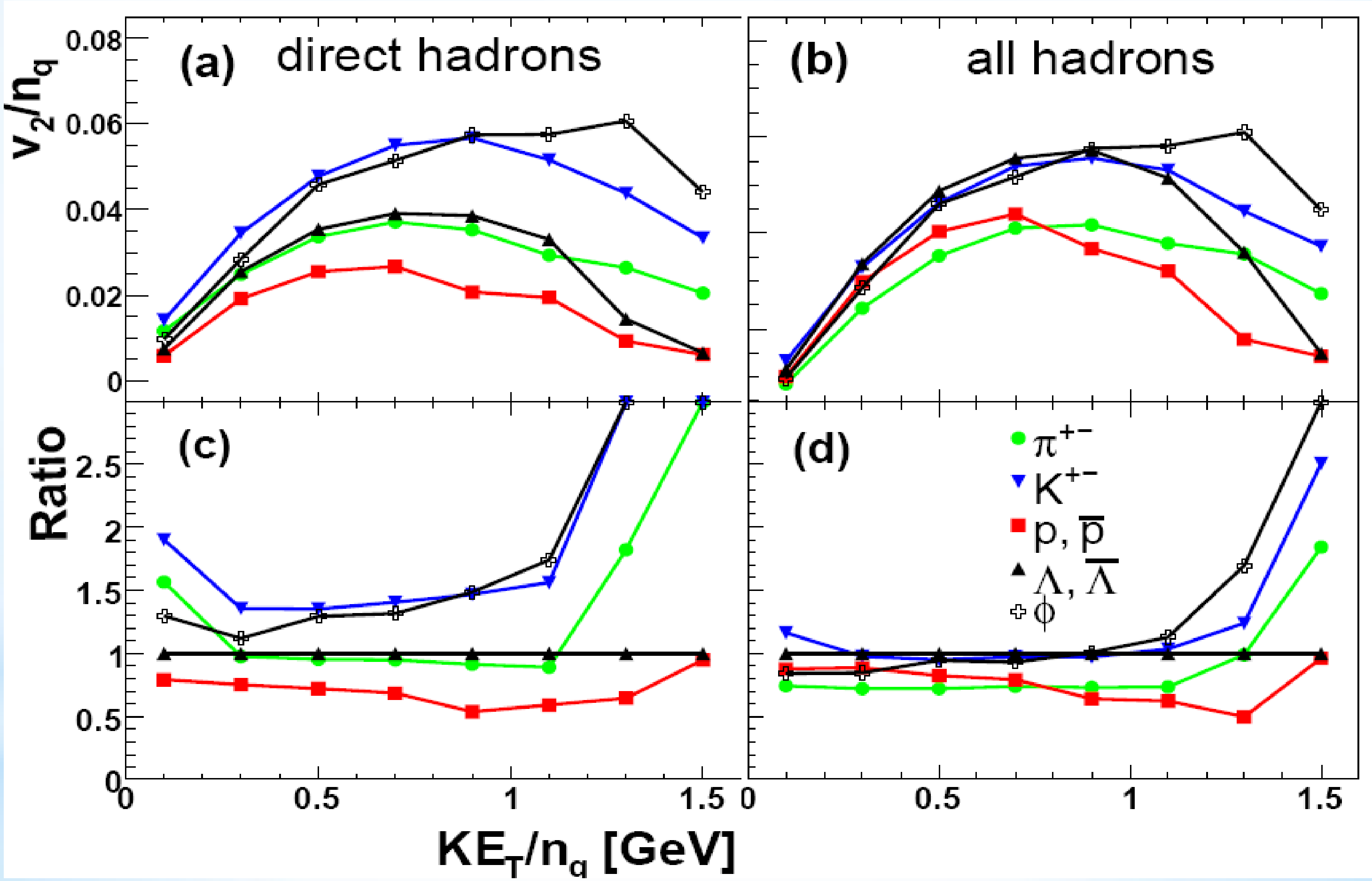

G.Eyyubova et al., PRC 80 (2009) 064907

LHC: NCQ scaling will be only approximate (prediction, 2009)

Experimental results (LHC)

ALICE Collaboration, M. Krzewicki et al., JPG 38 (2011) 124047

Semi-sentral collisions

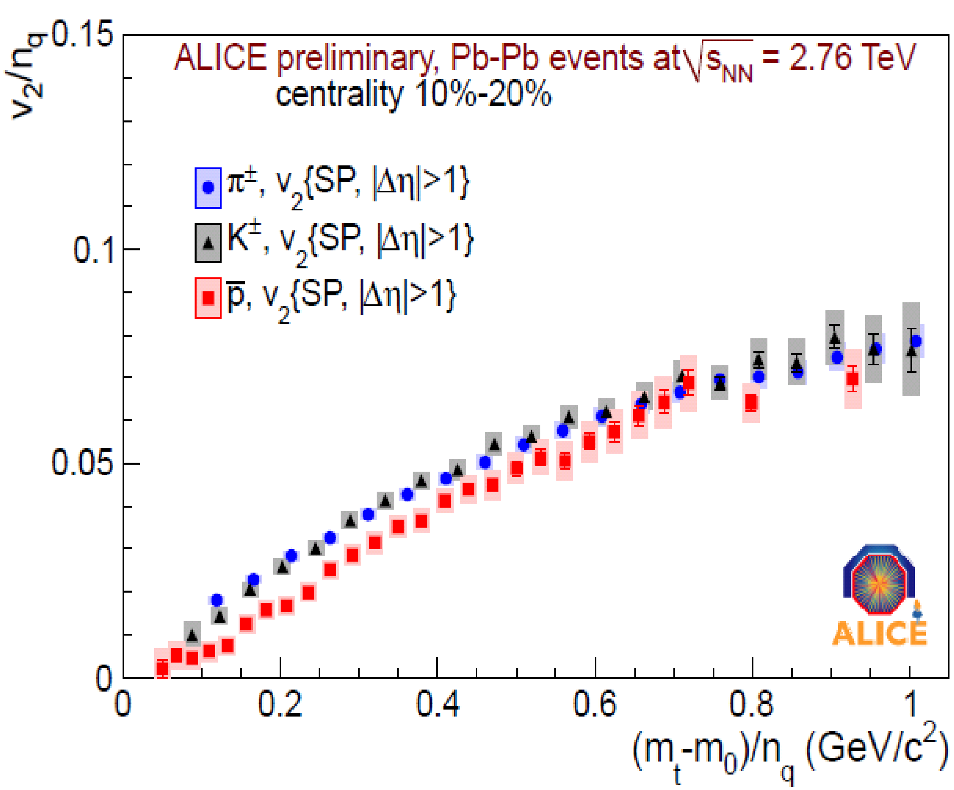

Semi-peripheral collisions

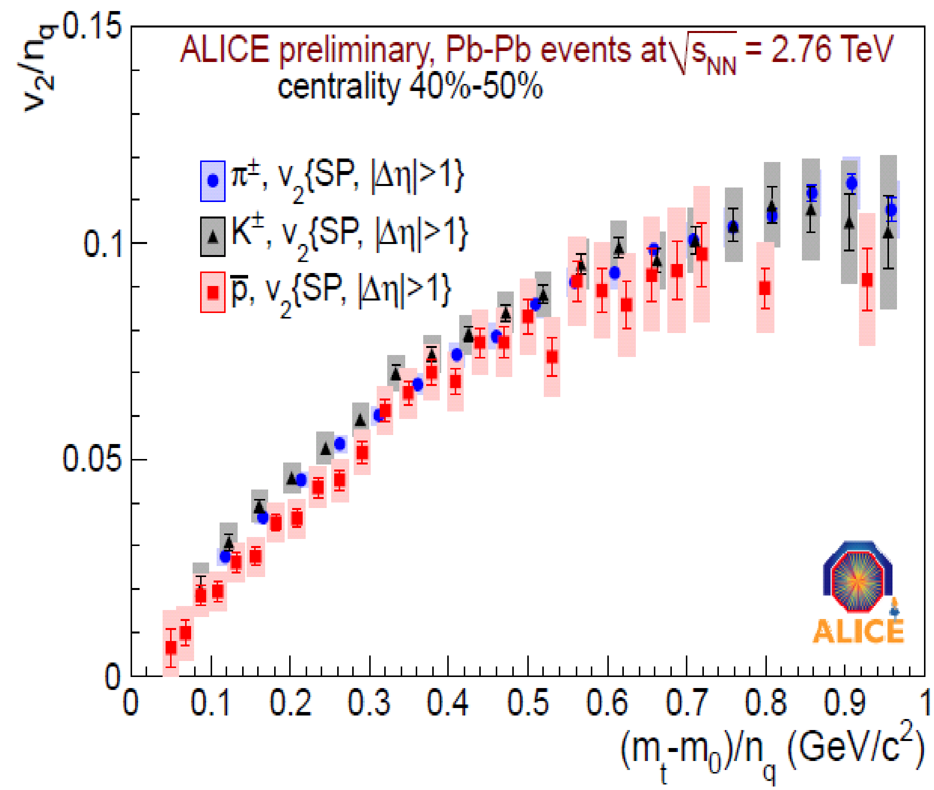

The NCQ scaling is indeed only approximate (2011)

NCQ-scaling of elliptic flow at beam energy scan (RHIC)

STAR Collab., PRL 110 (2013) 142301

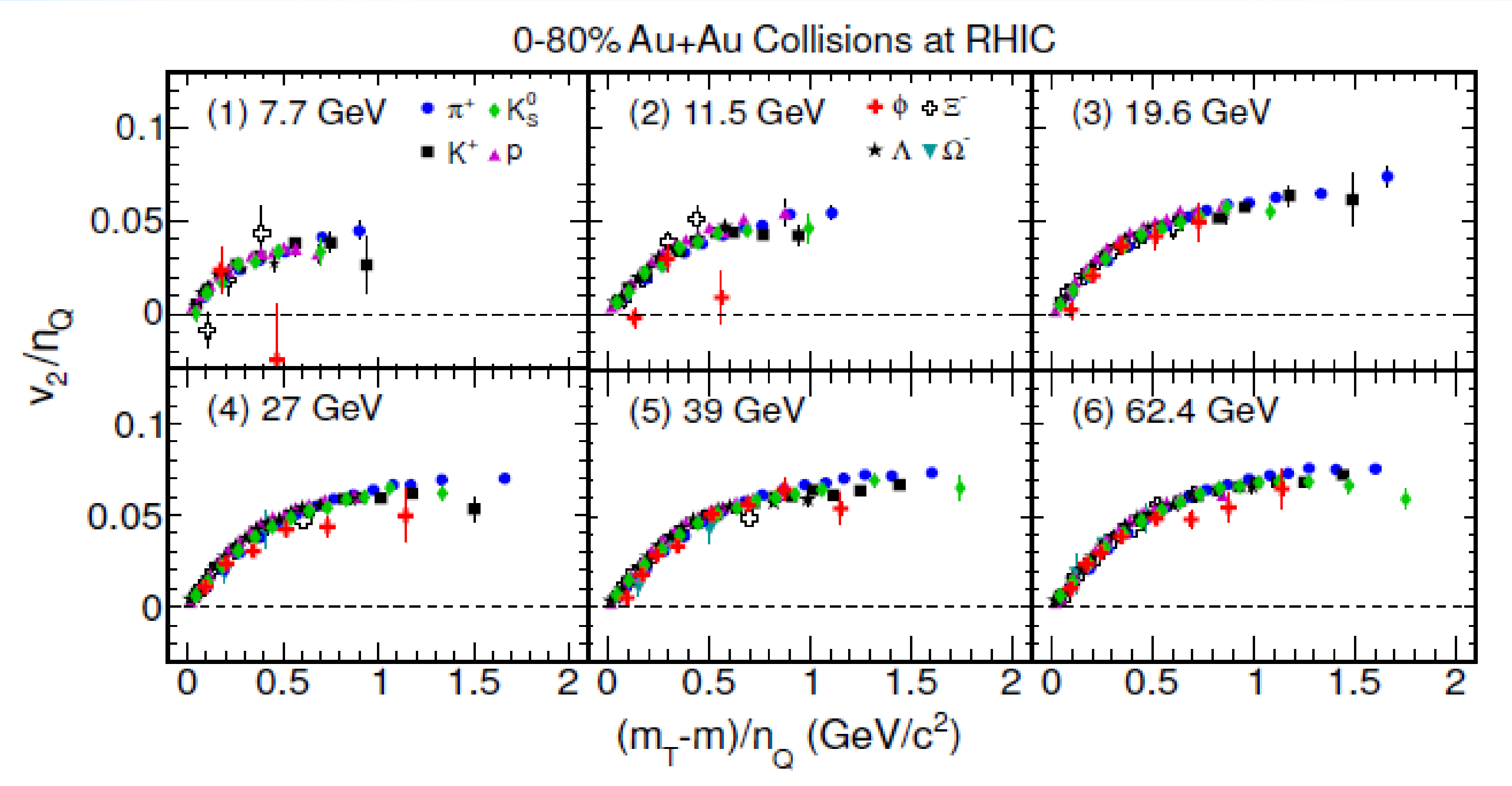

- NCQ scaling holds for particles and anti-particles separately at lower energies

Our explanation: jets (more influental at higher energies) violate the NCQ-scaling, whereas Hydro+Resonances work towards its fulfilment

V. Triangular flow

TRIANGULAR FLOW

B. Alver and G.Roland, PRC 81 (2010) 054905

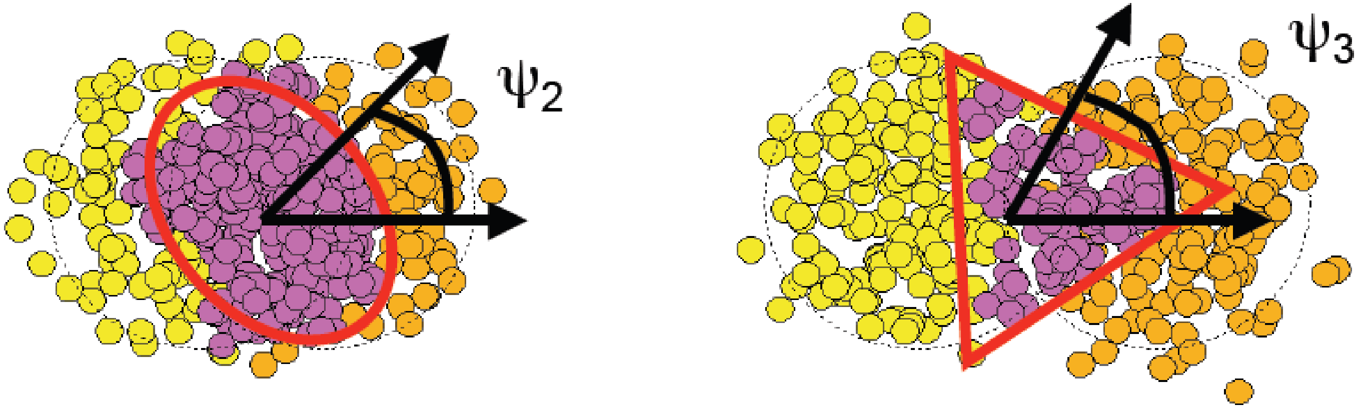

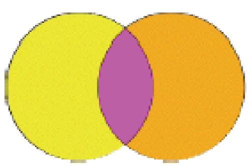

$$\frac{dN}{d\phi} = \frac{N}{2\pi}\left(1 + \sum 2v_n \cos\left(n(\phi - \psi_R)\right)\right)$$

$$v_2 = \left\langle \cos\left(2(\phi - \psi_R)\right)\right\rangle$$

$$v_3 = 0$$

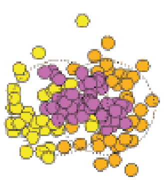

$$\frac{dN}{d\phi} = \frac{N}{2\pi}\left(1 + \sum 2v_n \cos\left(n(\phi - \psi_n)\right)\right)$$

$$v_2 = \left\langle \cos\left(2(\phi - \psi_2)\right)\right\rangle$$

$$v_3 = \left\langle \cos\left(3(\phi - \psi_3)\right)\right\rangle$$

The triangular initial shape leads to triangular hydrodynamic flow

Generation of triangular flow

V2

V3

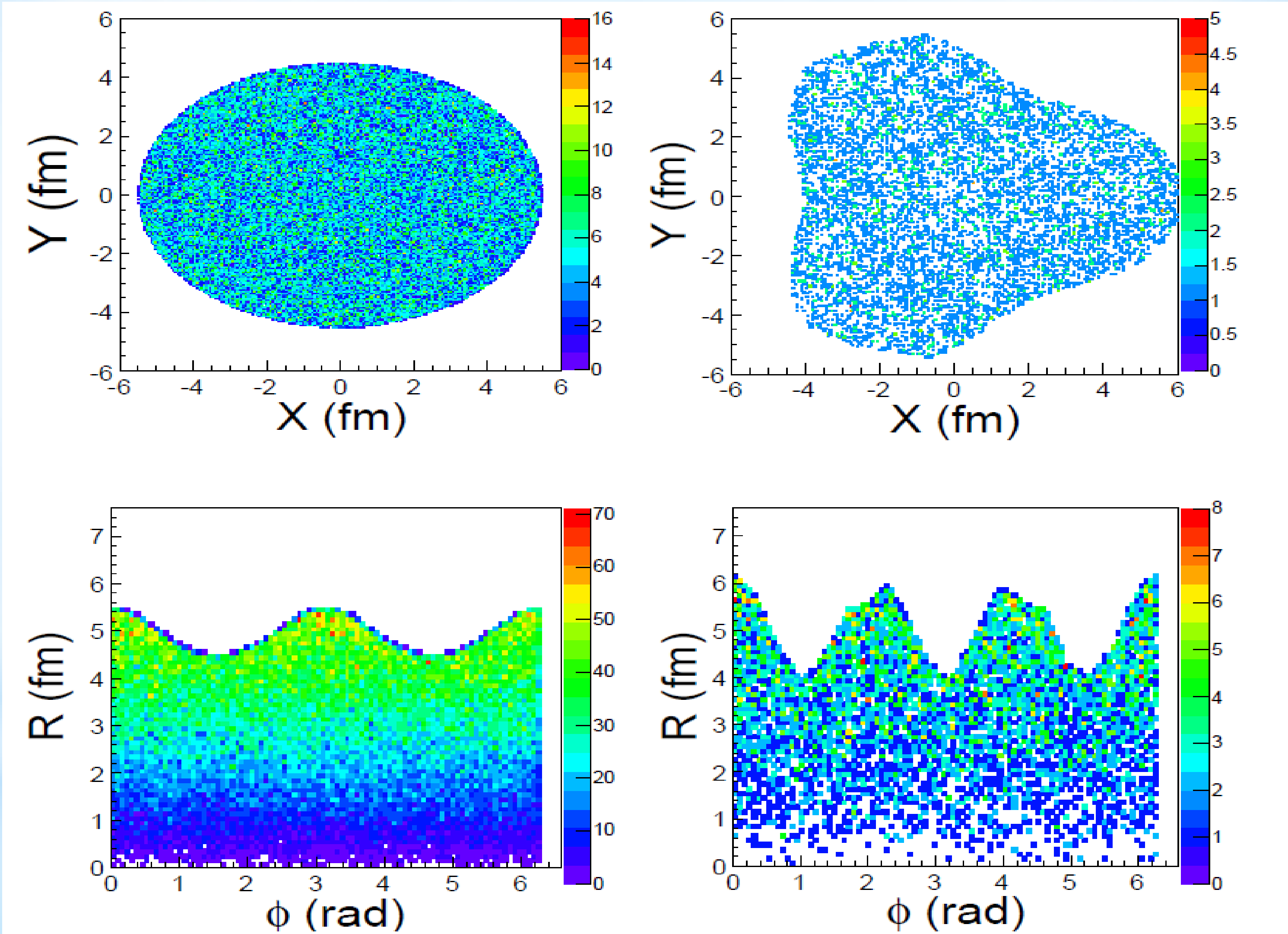

$$R(b,\phi) = R_f(b)\frac{\sqrt{1-\epsilon^2(b)}}{\sqrt{1+\epsilon(b)\cos 2\phi}}[1+\epsilon_3(b)\cos 3(\phi+\Psi_3^{\mathrm{RP}})]$$

LHC data vs. HYDJET++ model

Triangular flow

Pb+Pb @ 2.76 ATeV

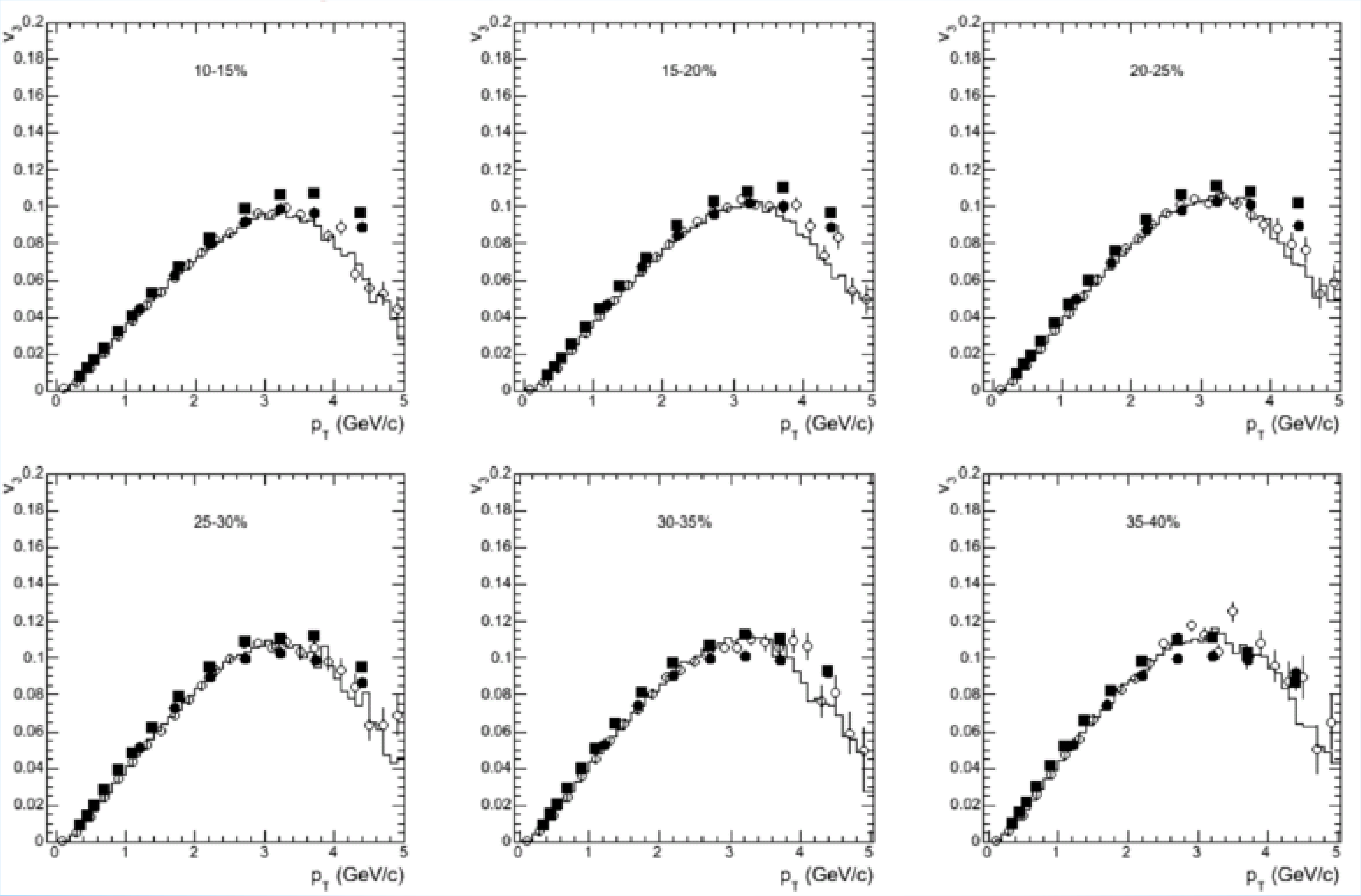

L. B. et al., Eur. Phys. J C74 (2014) 2807

VI. Higher flow harmonics

HIGHER FLOW HARMONICS

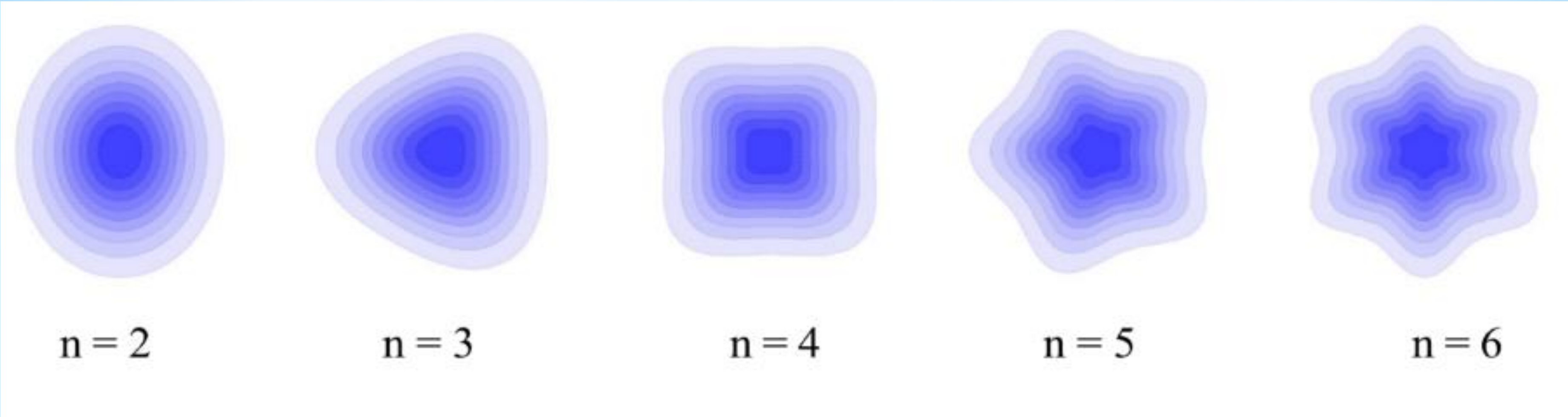

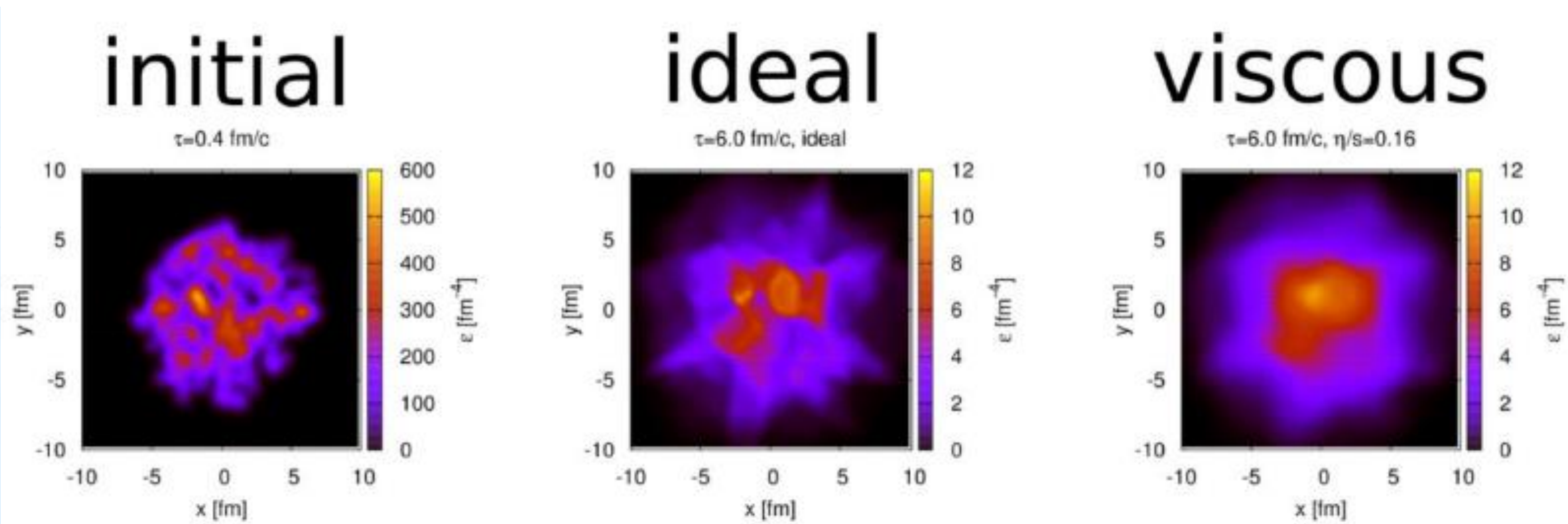

Non-zero higher Fourier coefficients can carry important information about the space-time evolution of the QCD-matter and initial fluctuations

CROSS-TALK BETWEEN FLOW HARMONICS

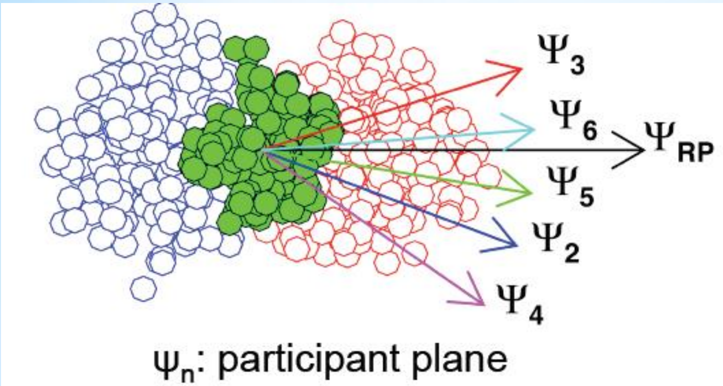

G.-Y. Qin et al, PRC 82 (2010) 064903

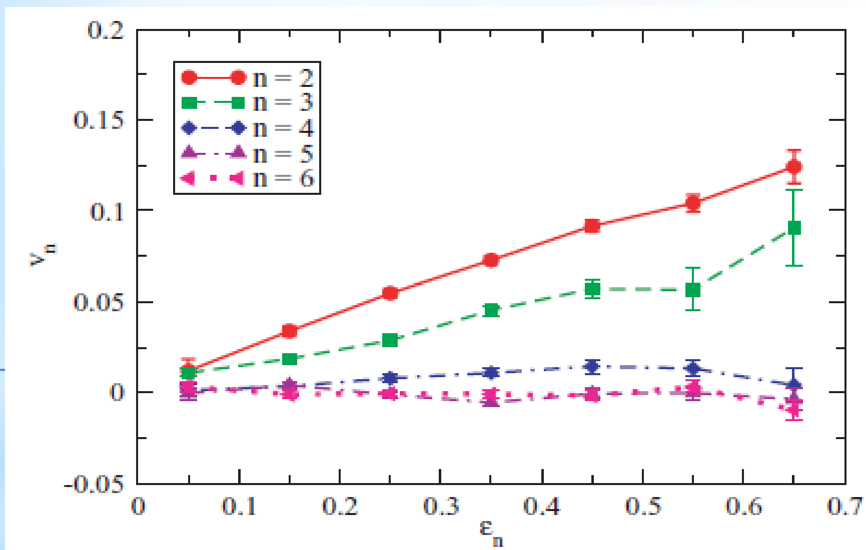

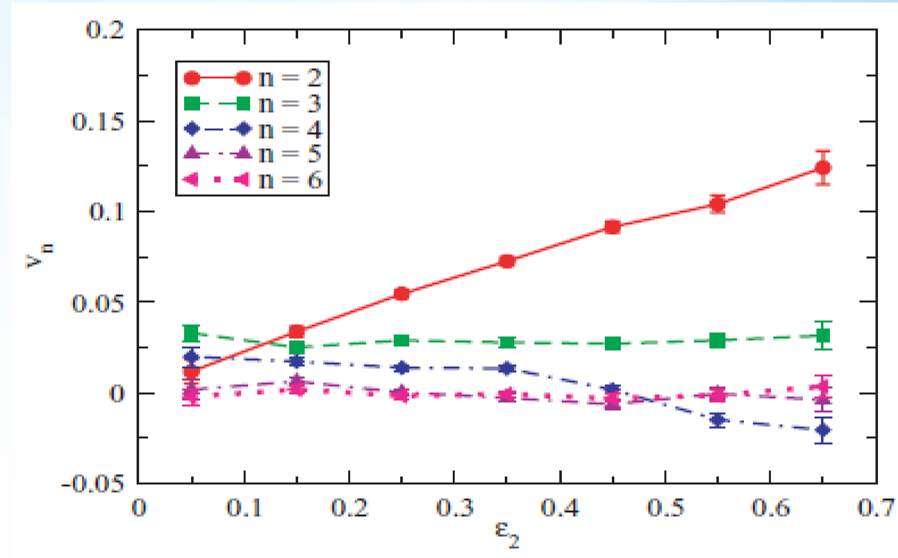

$$\begin{pmatrix} v_2 \\ v_3 \end{pmatrix} = \begin{pmatrix} M_{22} & M_{23} \\ M_{32} & M_{33} \end{pmatrix} \begin{pmatrix} \epsilon_2 \\ \epsilon_3 \end{pmatrix}$$

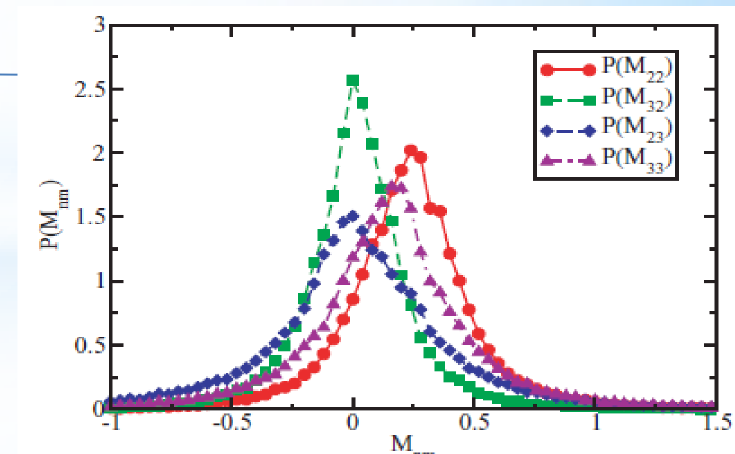

Only the first few flow harmonics of final-state hadrons survive after hydrodynamic evolution

LHC data vs. HYDJET++ model

Quadrangular flow

Pb+Pb @ 2.76 ATeV

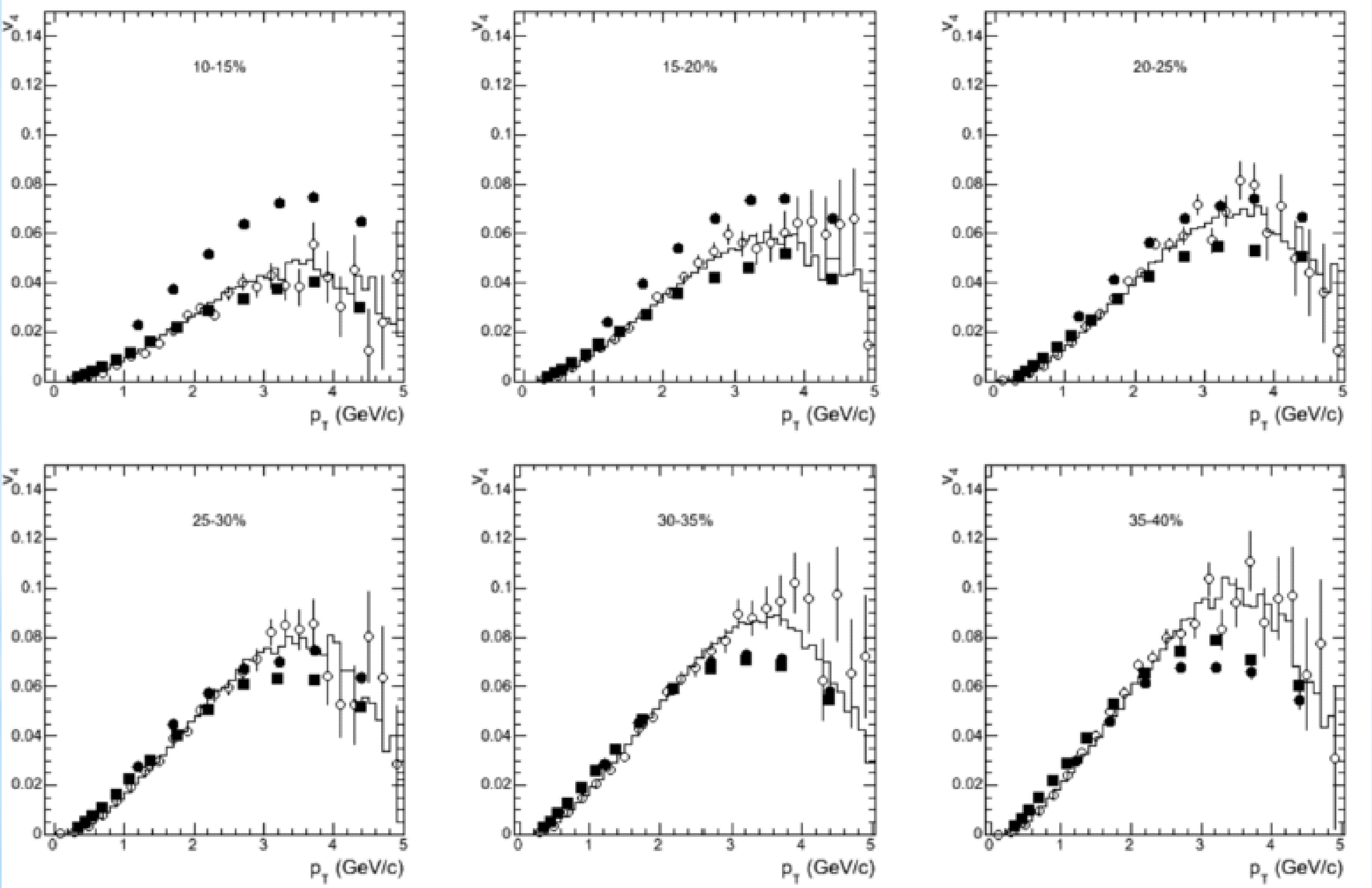

L. B. et al., Eur. Phys. J C74 (2014) 2807

v4 appears because of v2

LHC data vs. HYDJET++ model

Pentagonal flow

Pb+Pb @ 2.76 ATeV

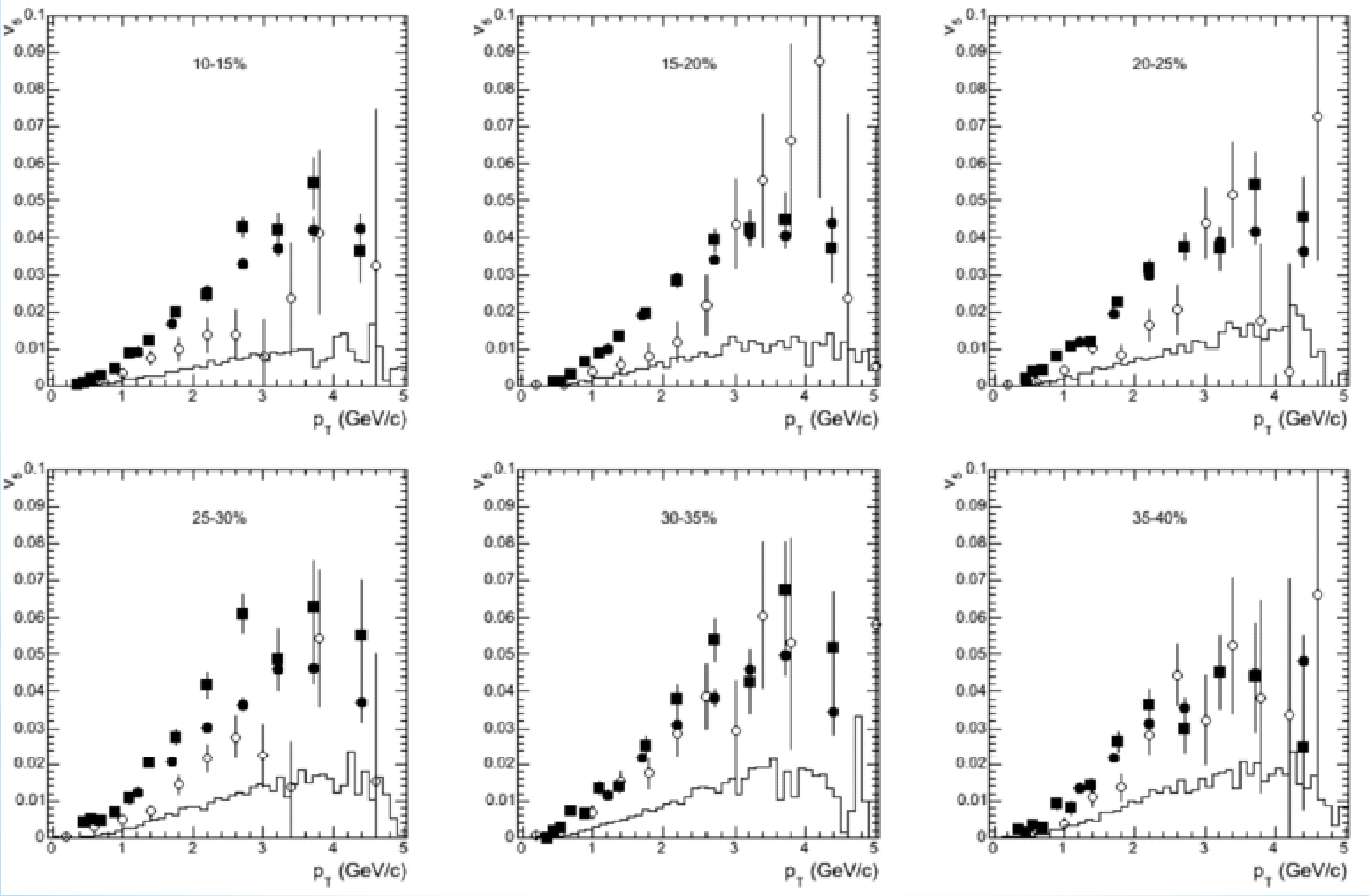

L. B. et al., Eur. Phys. J C74 (2014) 2807

v5 appears as product of v2 and v3 (no v2 or v3, no v5)

LHC data vs. HYDJET++ model

Hexagonal flow

Pb+Pb @ 2.76 ATeV

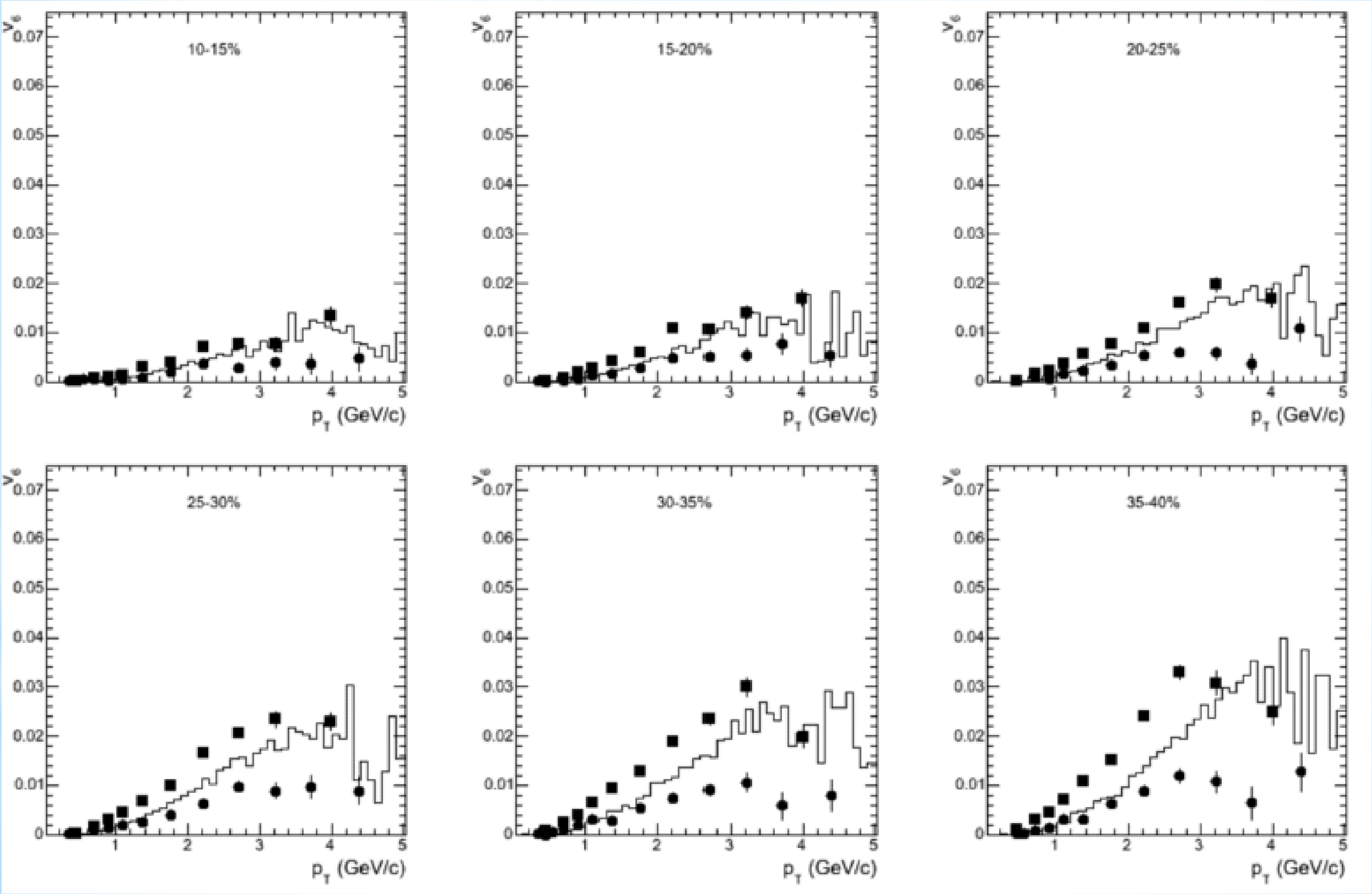

L. B. et al., Eur. Phys. J C74 (2014) 2807

Independent contributions from both v2 and v3

Hexagonal flow: $V_6 \propto \alpha V_2^3 + \beta V_3^2$

L. B. et al., PRC 89, 024909 (2014)

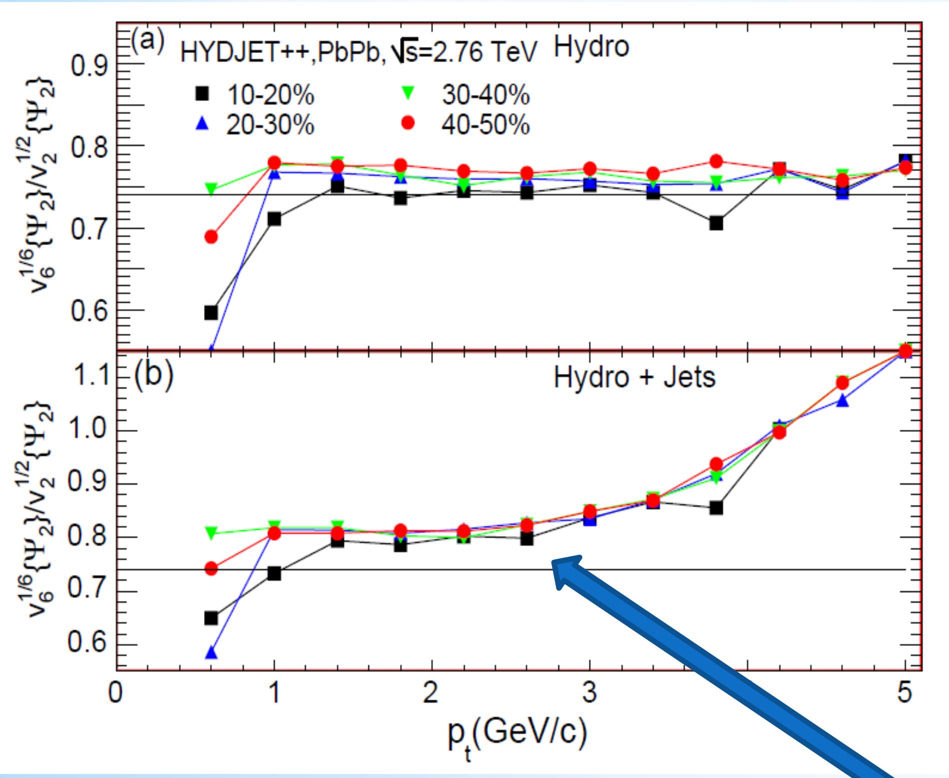

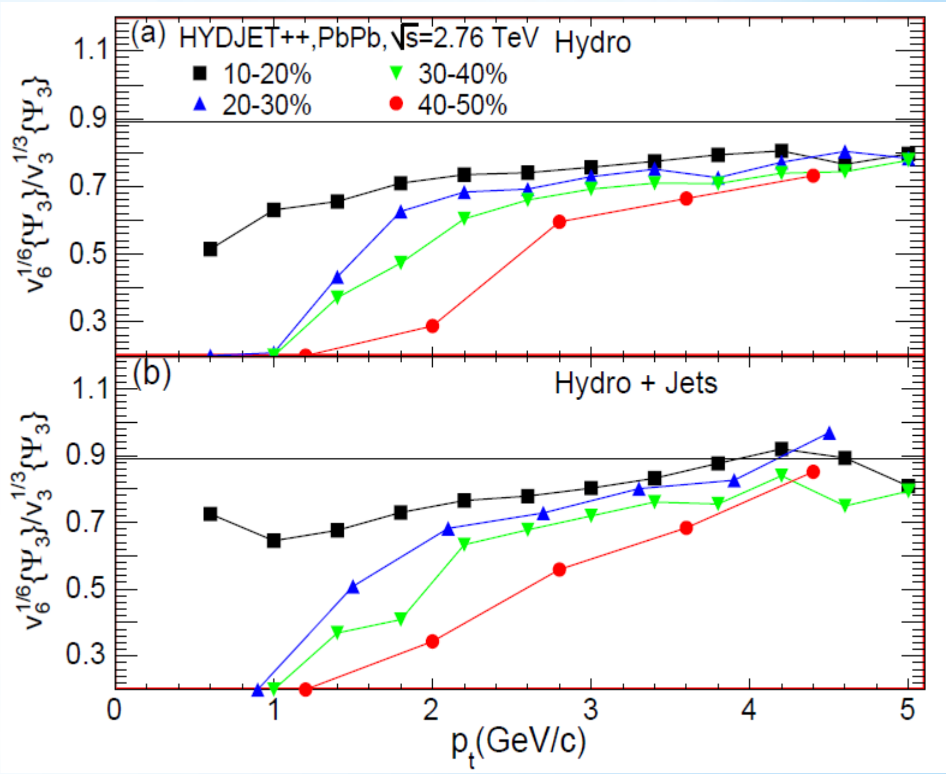

Ψ_2 Scaling? Ψ_3

It would be interesting to study $V_6(\Psi_2)$ and $V_6(\Psi_3)$ in experiment

Hexagonal flow: centrality dependence

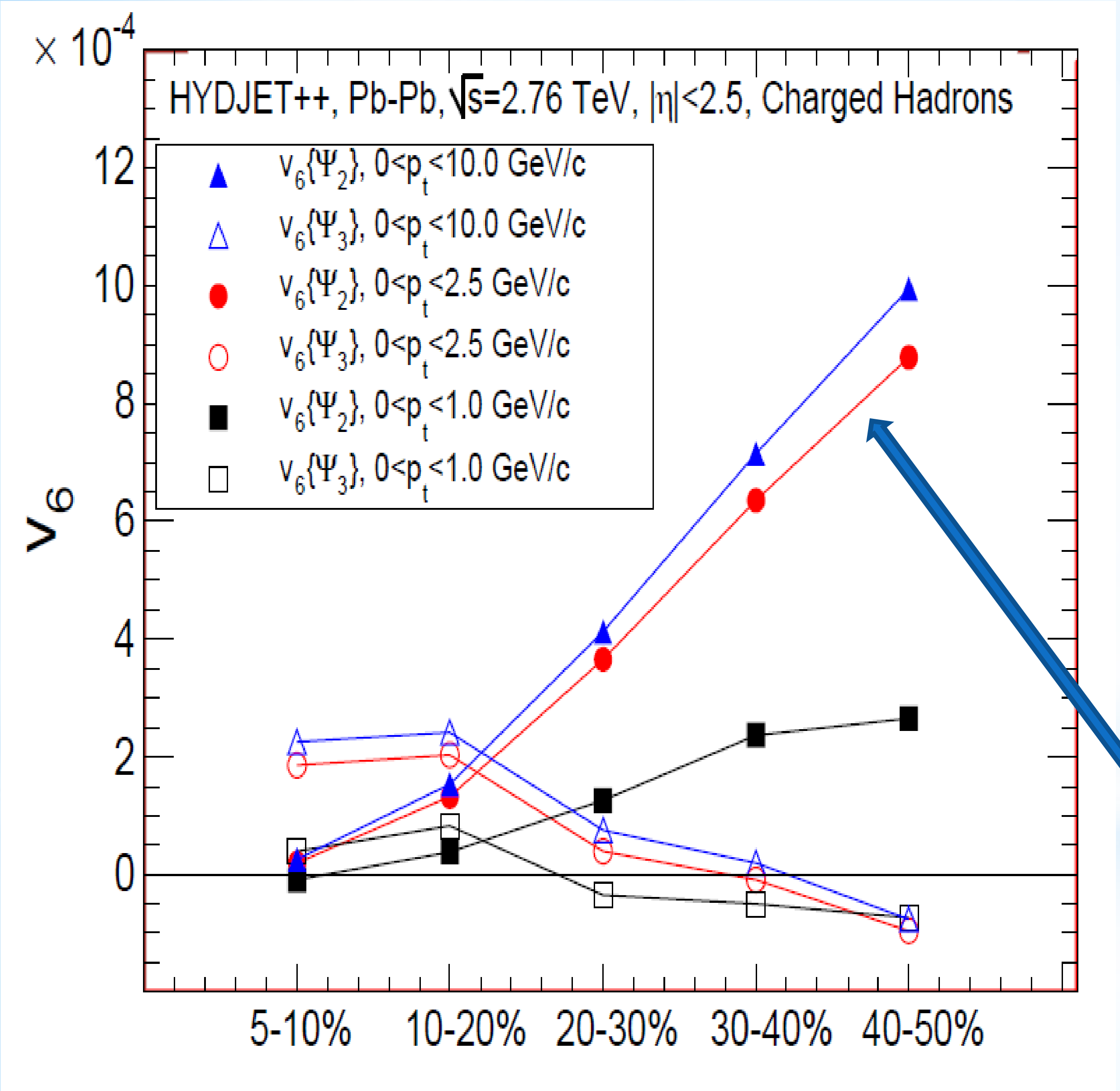

CMS Collab., PRC 89, 024909 (2014)

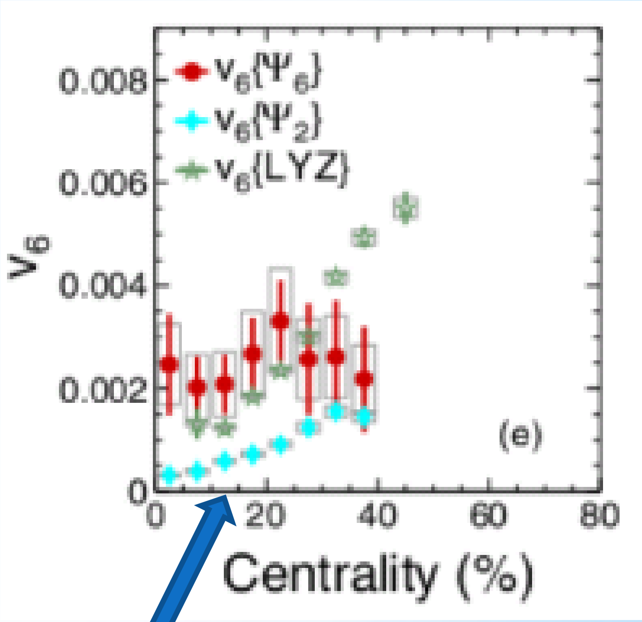

Centrality dependence in HYDJET++ is correct

Ridge – an interplay of v2 and v3?

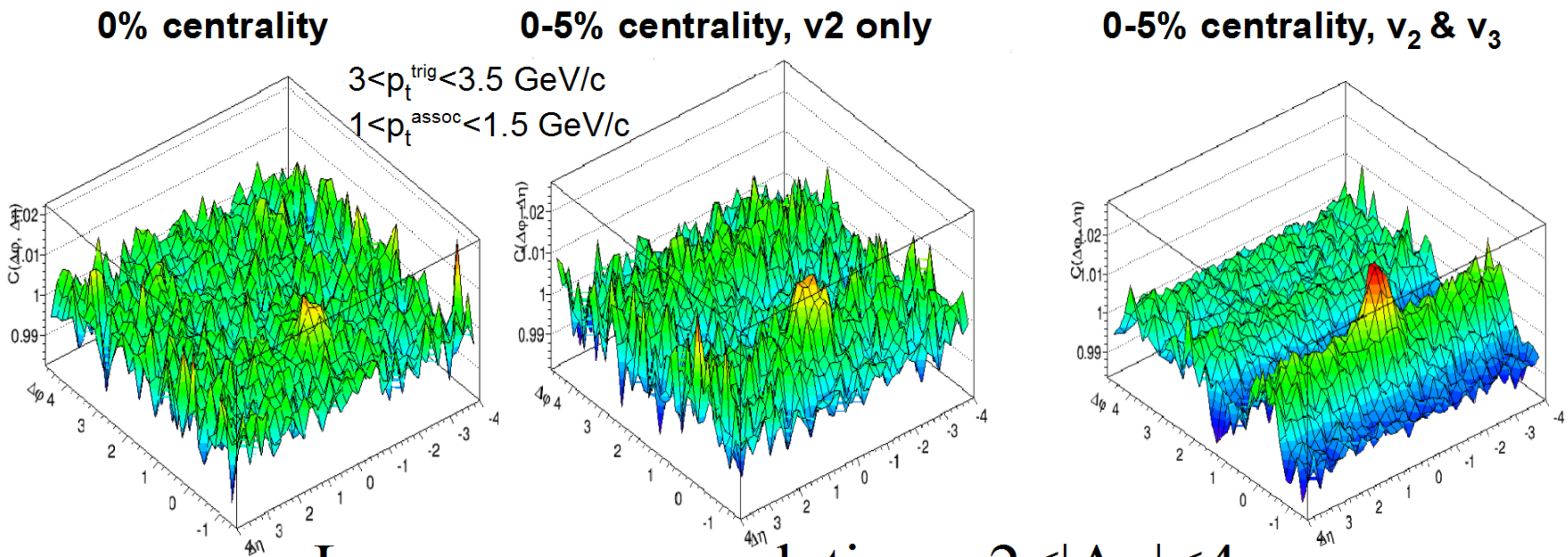

2D

Long range correlations, $2<|\Delta\eta|<4$

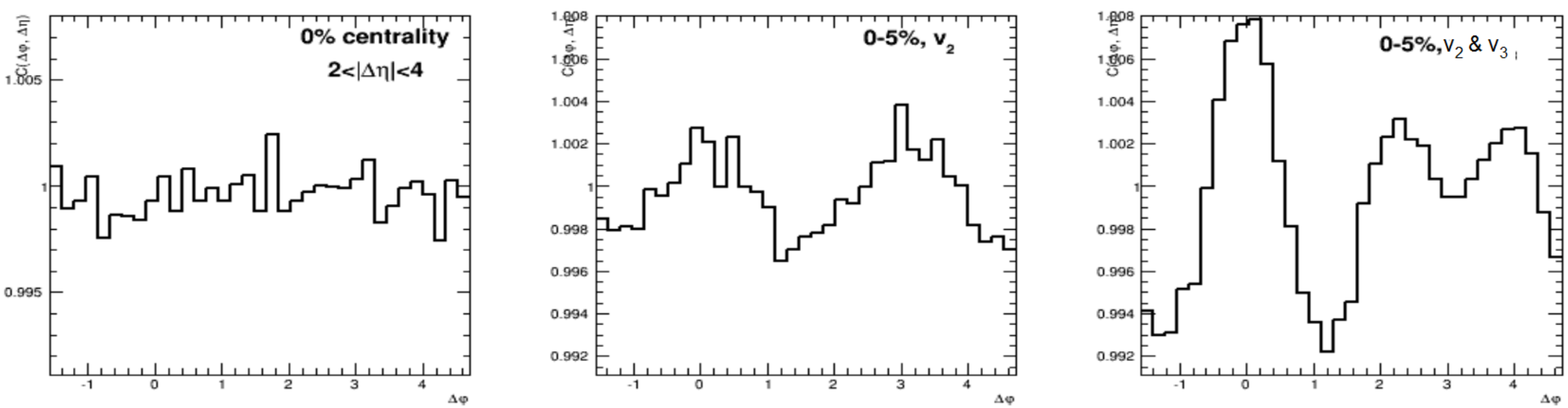

1D

G. Eyyubova et al., in preparation

- Long-range correlations appear due to flow.
- v_3 leads to double-peak structure at away side over Δφ.

CONCLUSIONS

The HYDJET++ model allows us to investigate flow of hydro and jet parts separately, to look at reconstruction of pure hydro flow and its modification due to jet part.

- ***HYDJET++ permits us to study cross-talk of v2 and v3, while other harmonics are absent***
- ***If only v2 is present, only even harmonics appear; odd harmonics arise if v3 is included***
- ***Scaling of v6^(1/6){psi2}/v2^(1/2){psi2} is predicted***
- ***Jets result to increase by 10%-15% of this ratio and lead to rise of its high-pT tail***
- ***Significant part of hexagonal flow and other higher order harmonics comes from elliptic and triangular flows***
- ***Ridge also appears in the model as a result of interplay of v2 and v3***

Back-up Slides

LHC data vs. HYDJET++ model

Pb+Pb @ 2.76 ATeV

Transverse momentum

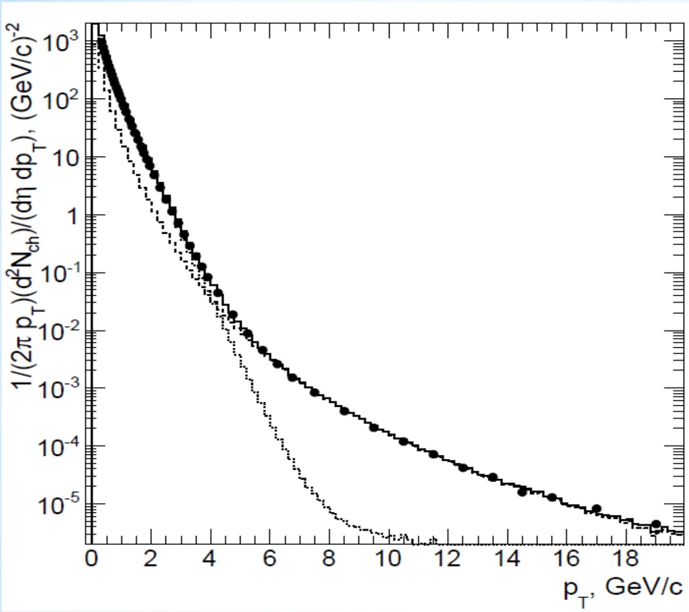

Rapidity

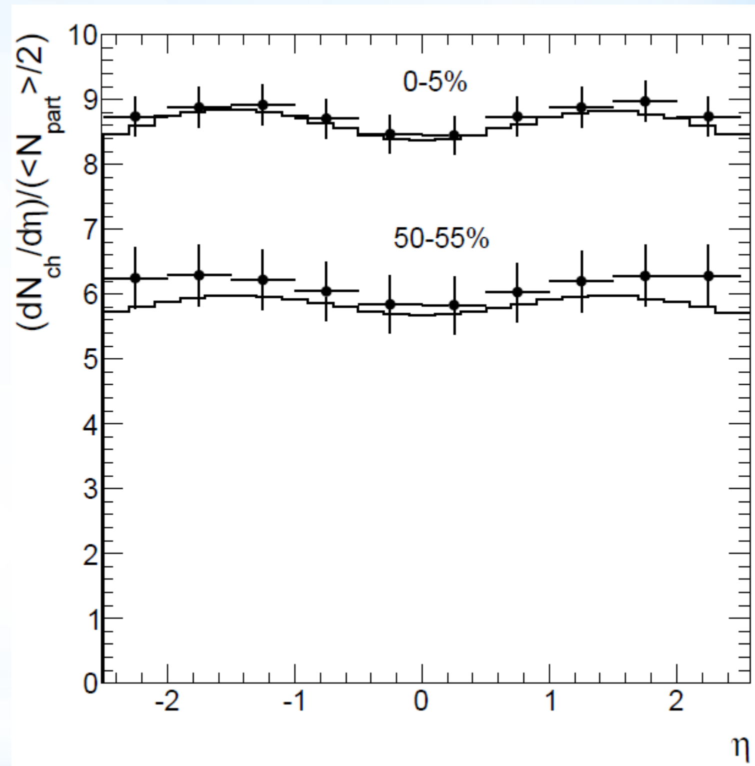

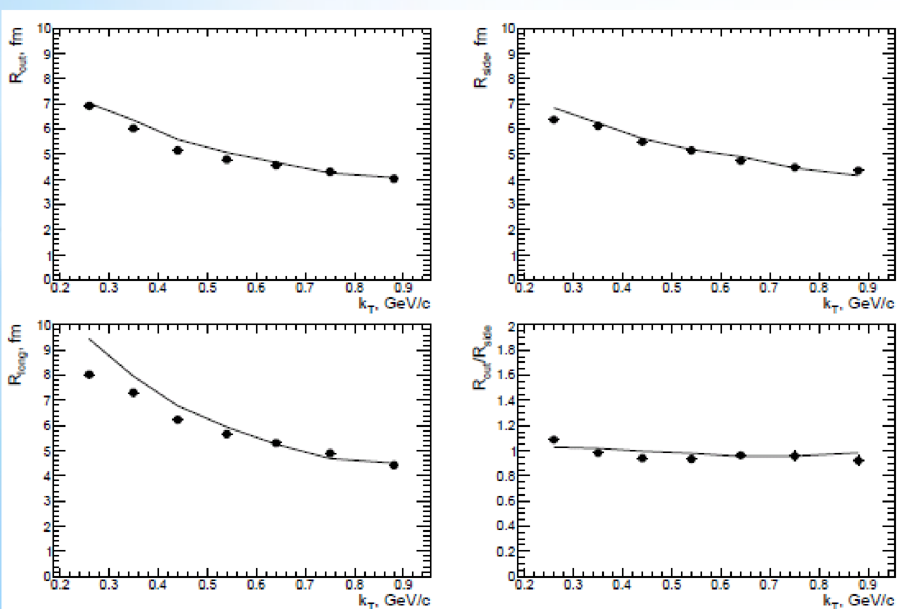

Correlation radii (femtoscopy)

I. Lokhtin et al., Eur. Phys. J C72 (2012) 2045

HYDJET++ results for RHIC

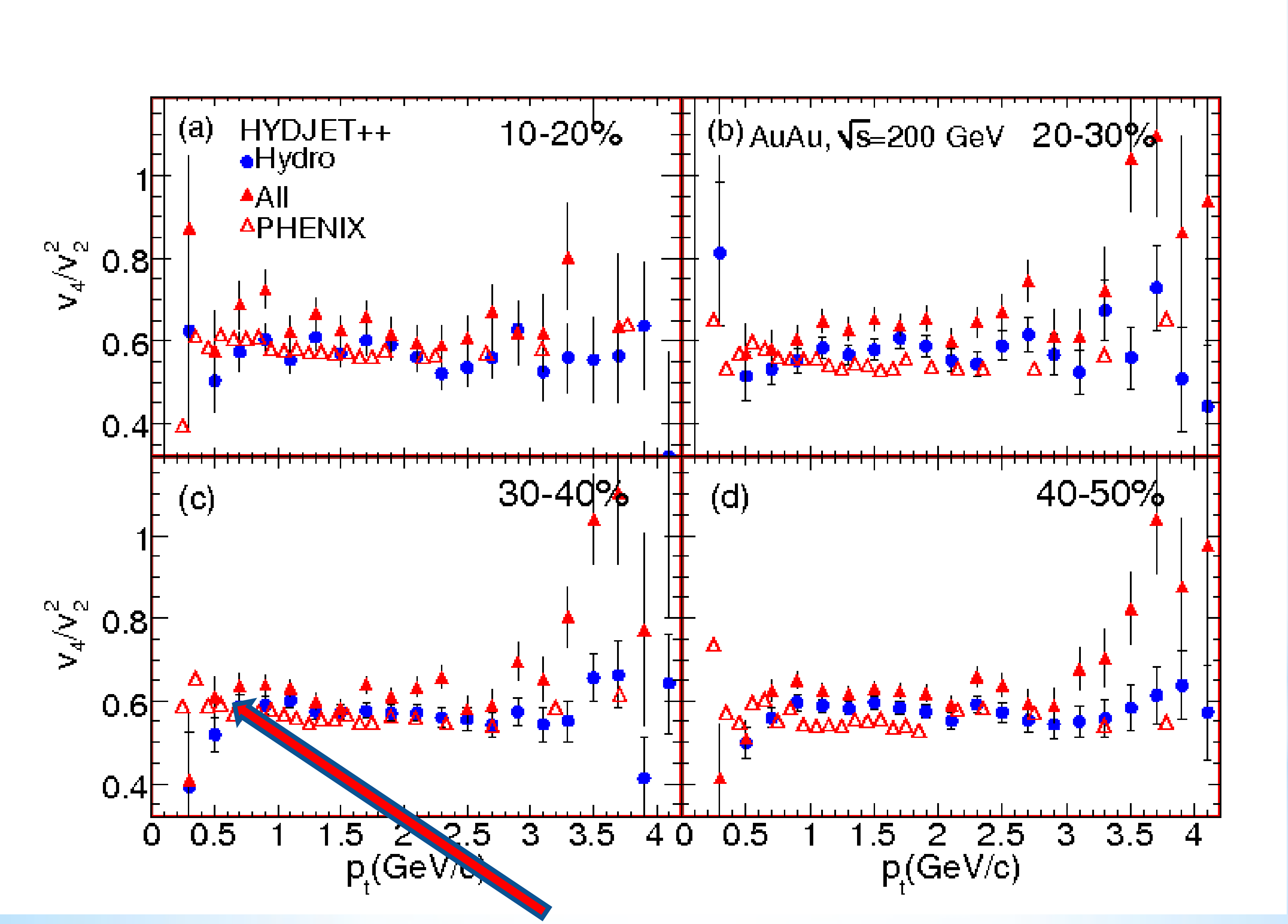

L.B. et al., PRC 80 (2013) 064907

Jets increase the ratio

HYDJET++ RESULTS for LHC

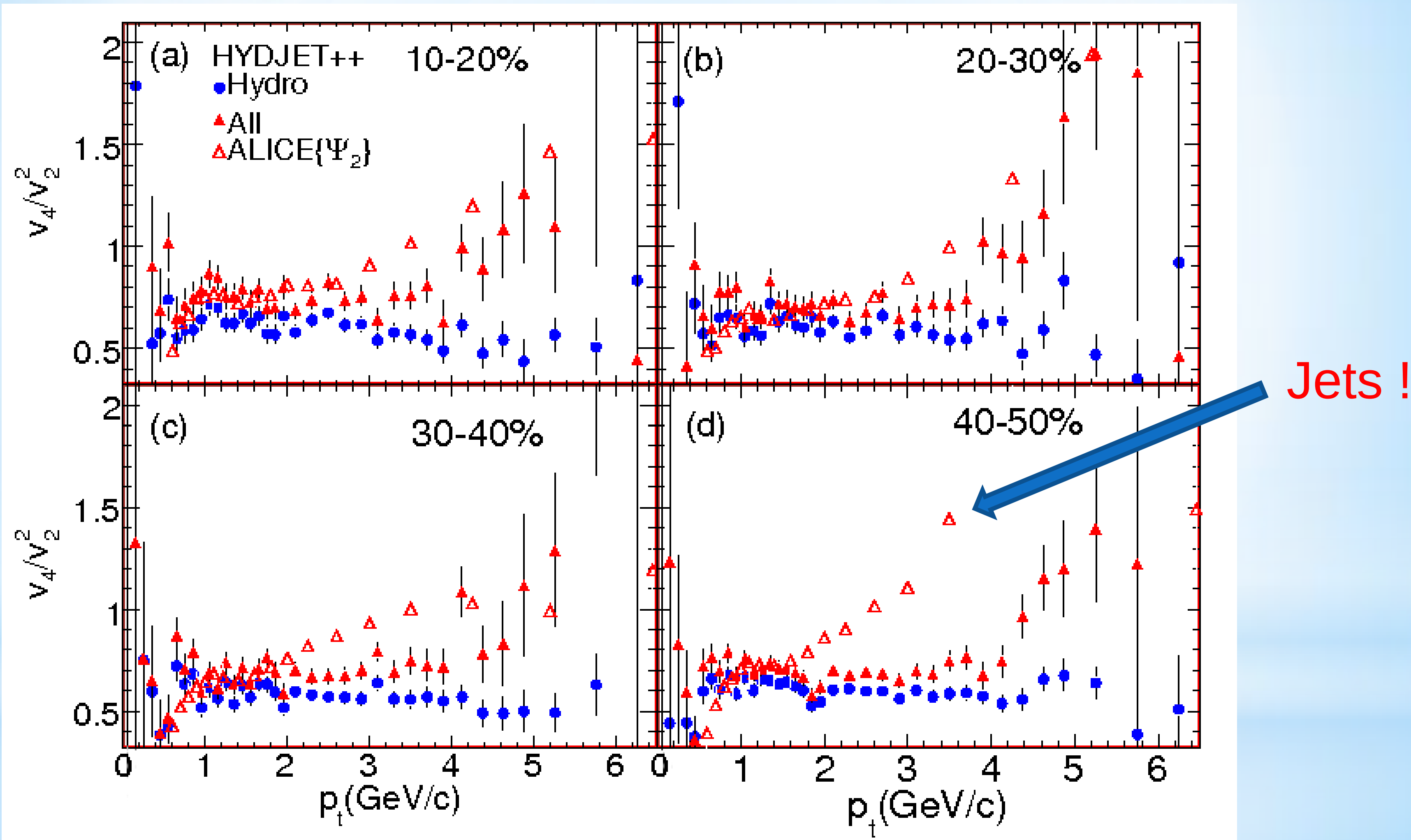

The same tendency is observed in Pb+Pb at LHC

Methods for **v2** calculation

(1) Event plane method

$$v_2^{obs}\{EP\} = \langle \cos 2(\varphi_i - \Psi_2) \rangle$$

$\Psi 2$ is the calculated reaction plane angle: $$\tan n\psi_n = \frac{\sum_i \omega_i \sin n\varphi_i}{\sum_i \omega_i \cos n\varphi_i}, \quad n \geq 1, \quad 0 \leq \psi_n < 2\pi / n$$

$$v_2\{EP\} = \frac{v_2^{obs}\{EP\}}{R} = \frac{v_2^{obs}\{EP\}}{\langle \cos 2(\Psi_2 - \Psi_R) \rangle}$$

(2) Two particle correlation method $$v_2\{2\} = \sqrt{\langle \cos 2(\varphi_i - \varphi_j) \rangle}$$

(3) Lee-Yang zero method $$G(ir) = \langle e^{irQ} \rangle, Q = \sum \cos(2\varphi)$$

Integral v2 is connected with the firs minimum r0 of the module of the G(ir):

$$v_2 = \frac{j_0}{Nr_0}$$

Differential flow is calculated by the formula: $$\frac{v_2(p_T)}{Nv_2} = \mathrm{Re}\left(\frac{\langle \cos(2\varphi) e^{ir_0 Q} \rangle}{\langle Q e^{ir_0 Q} \rangle} \right)$$

Comparison of Event Plane and Lee-Yang zeroes methods (c=30%)

EventPlane method

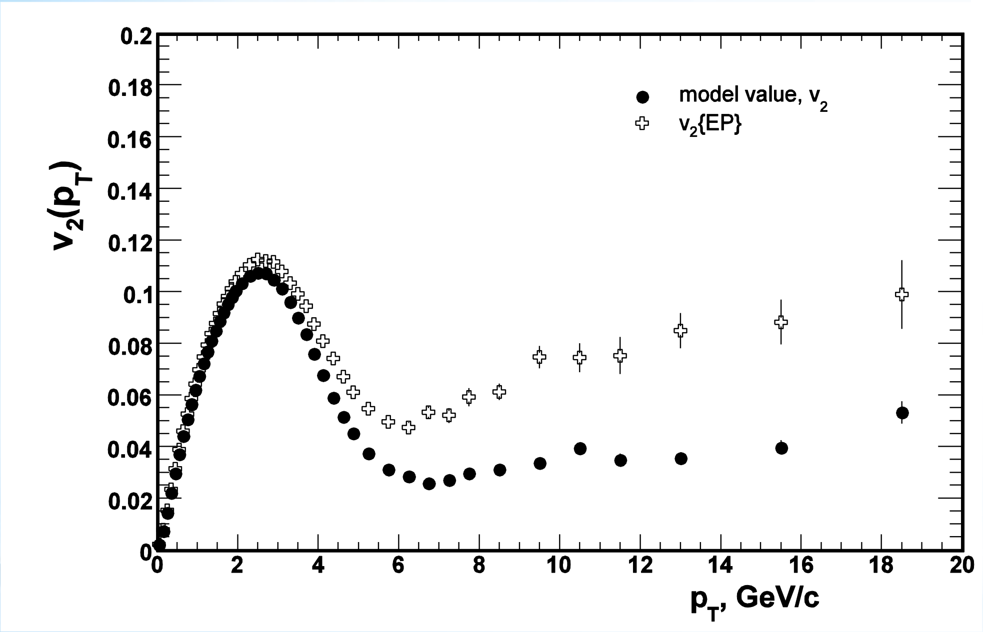

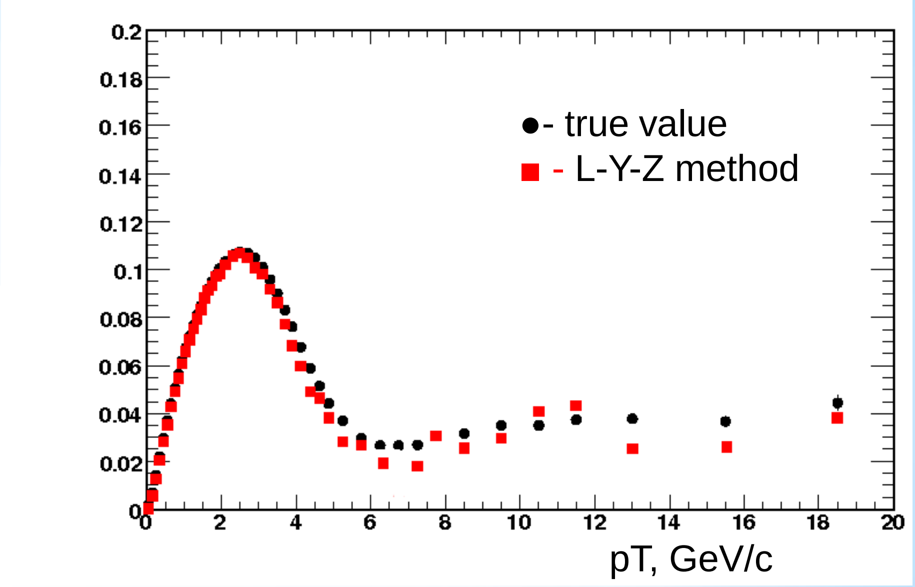

Lee-Yang zeroes Method

Event Plane method overestimates v2 at high pt due to non-flow correlation (mostly because of jets).